

This item is the archived peer-reviewed author-version of:

Biophysical drivers of the carbon dioxide, water vapor, and energy exchanges of a short-rotation poplar coppice

Reference:

Zenone Terenzio, Fischer Milan, Arriga Nicola, Broeckx Laura, Verlinden Melanie, Vanbeveren Stefan, Zona Donatella, Ceulemans Reinhart.- Biophysical drivers of the carbon dioxide, water vapor, and energy exchanges of a short-rotation poplar coppice

Agricultural and forest meteorology - ISSN 0168-1923 - 209(2015), p. 22-35

DOI: <http://dx.doi.org/doi:10.1016/j.agrformet.2015.04.009>

1 Biophysical drivers of the carbon dioxide, water vapor, and energy exchanges of a
2 short-rotation poplar coppice

3
4
5 Terenzio Zenone^a, Milan Fischer^b, Nicola Arriga^a, Laura S. Broeckx^a, Melanie S. Verlinden^a,
6 Stefan Vanbeverem^a, Donatella Zona^c and Reinhart Ceulemans^a

7
8
9
10
11
12 *^aDepartment of Biology, Research Centre of Excellence of Plant and Vegetation Ecology,
13 University of Antwerp, B-2610 Wilrijk Belgium*

14 *^bGlobal Change Research Center AS CR, v.v.i., Bělidla 986/4a, 603 00, Brno, Czech Republic*

15 *^cDepartment of Animal and Plant Sciences, University of Sheffield, United Kingdom*

16
17
18
19
20 Corresponding author: Dr. Terenzio Zenone.

21 University of Antwerp, Department of Biology, Universiteitsplein 1, B-2610 Wilrijk, Belgium

22 E-mail: Terenzio.Zenone@uantwerpen.be

23 Phone + (32) 3-265-2831; Fax: + (32) 3-265 2271.

24
25
26
27 Keywords: bioenergy crop, carbon uptake, evapotranspiration, surface conductance, leaf area
28 index, Omega factor, decoupling

34 Abstract

35 We used the eddy-covariance technique to measure the temporal dynamics and the relationships
36 between leaf area index (LAI) and exchanges of carbon dioxide (CO₂), latent heat (LE) and
37 sensible heat (H) in a multi-genotype short-rotation poplar coppice (SRC) located in East-
38 Flanders (Belgium). The study was carried out over four years (2010-2013) corresponding to the
39 first two rotations of the plantation. The net carbon (C) balance during the first two-year rotation
40 was 75.2 (± 4.4) g C m⁻² in the establishment year 2010 and -95.6 (± 5.9) g C m⁻² in 2011. After
41 the harvest (second two-year rotation) the coppice was a net source of carbon, 151.0 (± 10.5) g C
42 m⁻² in 2012, but a sink of -274.6 (± 18.8) g C m⁻² in 2013. Overall, at the end of the second
43 rotation this SRC, was a net CO₂ sink with a cumulative uptake of -144.0 (± 22.8) g C m⁻². The
44 temporal dynamics and the magnitude of the ratio between gross primary production (GPP) and
45 ecosystem respiration (R_{eco}) were similar to a deciduous forest. The evolution of LAI showed
46 values ranging from 0.96 (± 0.4) to 2.0 (± 1.2) and from 5.1 (±1.5) to 4.5 (± 0.84) during the first
47 and the second rotation, respectively. The GPP (measured close to light saturation) was
48 significantly related to LAI (r² of 0.76, p < 0.001). The cumulative evapotranspiration (ET)
49 measured during the first rotation was 241.7 mm and 349.9 mm for 2010 and 2011 respectively,
50 and 464.6 mm and 372.1 mm for 2012 and 2013. The average value of surface conductance (G_s)
51 was 0.35 mol m⁻² s⁻¹ and 0.24 mol m⁻² s⁻¹ for the foliated and unfoliated periods, respectively.
52 The mean decoupling factors (Ω) were 0.35 and 0.23 for the foliated and unfoliated periods,
53 respectively, indicating that ET was primarily controlled by vapor pressure deficit (VPD) and G_s
54 (a well-coupled system). The mean Priestley-Taylor coefficient (α) was 0.77 and 0.53 for the
55 foliated and the unfoliated periods, respectively. Such low values indicate that ET was
56 significantly lower than the equilibrium evaporation and thus also lower than the ET of a
57 hypothetical reference crop. During the whole experiment only two short episodes of drought
58 were identified when in May-June 2011 and June 2013 the evaporative fraction dropped below
59 0.4. The analysis of G_s showed a rather low stomatal control (anisohydric stomatal response) that
60 put the poplar SRC at greater risk during severe drought conditions. All the three mentioned
61 parameters related to ET and GPP (G_s, Ω and α) were significantly and positively correlated to
62 LAI (r² from 0.14 to 0.2, p < 0.0001), suggesting that LAI was the main biophysical driver
63 controlling the carbon and water balances in this bioenergy production system.

64

65 1. Introduction

66

67 The European Union has set the target of increasing the use of renewable energy sources to at
68 least 20% of total consumption by the year 2020 (EU, 2009). The objective is to reduce the
69 consumption of fossil fuels and thereby reduce CO₂ emissions (Zetterberg *et al.*, 2014). Within
70 the context of the search for renewable energy sources dedicated lignocellulosic crops, as short-
71 rotation coppice (SRC), have a high potential. Indeed, one might expect a considerable increase
72 in the area of these SRC if they are to be used as conventional biofuel for bioenergy production,
73 or for the production of second-generation biofuels (Eisentraut, 2010). Poplar (*Populus spp.*) is
74 one of the genera that currently receives a lot of attention as a very suitable crop for the
75 production of biofuel (Kauter *et al.*, 2003; Aylott *et al.*, 2008, AEBIOM 2012). The carbon (C)
76 uptake by crops is primarily determined by the biology of the vegetation – e.g., leaf area index
77 (LAI), physiological activity, length of the growing season – as well as by the meteorological
78 conditions (Schmid *et al.*, 2000). The gross primary productivity (GPP) is primarily dependent
79 on the photosynthetically active radiation (PAR), in combination with LAI, while ecosystem
80 respiration (R_{eco}) strongly responds to air and soil temperature (Carrara *et al.*, 2004; Baldocchi,
81 1997; Reichstein *et al.*, 2002). Carbon uptake in SRC is considered to be very sensitive to low
82 water availability (Broeckx *et al.*, 2013), and to high temperatures by stomatal (increase of vapor
83 pressure deficit) and non-stomatal control (influencing R_{eco}) (Migliavacca *et al.*, 2009). This
84 suggests that SRC plantations could be vulnerable to climate change in regions where water is in
85 short supply (King *et al.*, 2013). Moreover, a poplar SRC might be more sensitive to drought
86 than other deciduous and coniferous forests because poplar is a fast-growing species with rather
87 low stomatal control (Pita *et al.*, 2013).

88 Monitoring the net ecosystem exchange (NEE) of CO₂ (and its partitioning into GPP and R_{eco}) in
89 combination with the fluxes of sensible heat (H) and latent heat (LE) is essential for quantifying
90 the carbon sequestration potential and water use of SRC plantations, as well as for identifying the
91 main environmental and/or biophysical drivers. Several studies on the physiology of SRC and of
92 longer-rotation poplar plantations have already tried to elucidate the environmental controls (e.g.,
93 Neumann *et al.*, 1996; Calfapietra *et al.*, 2003, 2005; Zona *et al.*, 2013). Heatwaves can induce a
94 considerable reduction of the net C uptake in longer rotation (twelve-year) poplar plantations,
95 even in the absence of pronounced soil water stress (Migliavacca *et al.*, 2009). On the other hand

96 in a two-year-old SRC plantation, soil water shortage limited the NEE when the water table
97 progressively decreased and vapor pressure deficit (VPD) became an important control on CO₂
98 fluxes. By removing the influence of solar radiation on NEE, VPD explained up to 16% of the
99 variability, and water limitation on CO₂ uptake mostly occurred when VPD was >1 kPa (Zona *et*
100 *al.* 2013).

101 Here, we present and discuss measurements of CO₂ and H₂O fluxes in combination with
102 measurements of LAI of a poplar SRC over a four-year period. We hypothesize that LAI
103 explains most of the variability of the eco-physiological parameters that drive the CO₂ and water
104 vapor exchanges. The knowledge of LAI is therefore useful to determine carbon uptake and
105 water use of poplar SRC under various environmental conditions. In terms of water
106 consumption of the SRC crop we hypothesized that the ET of the poplar plantation was lower
107 than the ET of an hypothetical reference crop. The objectives of the present study were: (i) to
108 quantify the magnitude and the seasonal dynamics of CO₂, water vapor and energy exchanges
109 during two two-year rotations for a poplar SRC; (ii) to investigate the role of LAI in controlling
110 GPP and ET; (iii) to quantify and analyze the seasonal variation of surface conductance (G_s),
111 decoupling factor (Ω), and Priestley-Taylor coefficient (α). These latter variables represent
112 important bulk parameters that treat the soil and the vegetation as one single layer, in relation to
113 LAI.

114

115 2. Material and Methods

116 2.1. Site description

117 The research site was an operational multi-genotype SRC plantation of poplars located in
118 Lochristi, East-Flanders (Belgium; 51°06'44" N, 3°51'02" E) at an elevation of 6.25 m above
119 sea level. The SRC culture was planted on 7-10 April 2010 with 12 selected genotypes of
120 *Populus deltoides*, *P. maximowiczii*, *P. nigra*, and *P. trichocarpa*, and their interspecific hybrids
121 in a double-row design with a planting density of 8000 plants ha⁻¹. No fertilizers and no
122 irrigation were applied during the four years of the study. The aboveground biomass was
123 harvested in January-February 2012 (end of the first rotation) and in February 2014 (end of the
124 second rotation). The first rotation was characterized by single-stem plants, while the second
125 rotation consisted a multiple-stem coppice. More details on the planting materials, and on the

126 plantation lay-out and management are provided by Broeckx *et al.* (2012) and Verlinden *et al.*
127 (2013).
128 The present contribution and the SRC plantation are part of the larger POPFULL project
129 (<http://uahost.uantwerpen.be/popfull>) where the full balances of greenhouse gases, of energy and
130 the economics are being evaluated. The 30-year average annual temperature and precipitation
131 (collected by a nearby station of the Royal Meteorological Institute of Belgium; www.meteo.be)
132 at the site are 9.5°C and 726 mm, respectively. The precipitation is equally distributed across the
133 year. The site is characterized by two different former land-use types: extensively grazed pasture,
134 and agricultural cropland (ryegrass, wheat, potato, beet, and most recently monoculture maize
135 with regular nitrogen (N) fertilization at a rate of 200-300 kg ha⁻¹ yr⁻¹ as liquid animal manure
136 and as chemical fertilizer).
137 Prior to planting a soil survey (described in detail by Broeckx *et al.*, 2012) revealed that the soil
138 has a sandy texture with a clay-enriched deeper soil layer and poor natural drainage. The carbon
139 (C) and N mass fractions were significantly different in the upper 0-15 cm soil layer ($p = 0.0001$)
140 and were lower in previous cropland ($1.48\% \pm 0.32$ and $0.12\% \pm 0.03$, respectively) as compared
141 to previous pasture ($1.95\% \pm 0.36$ and $0.18\% \pm 0.03$, respectively). The C and N contents – in
142 the upper 90 cm – were not significantly different between the two different former land-use
143 types (Broeckx *et al.*, 2012).

144

145 2.2. Flux and meteorological measurements

146

147 The eddy-covariance (EC) system – used to measure gas and energy fluxes between the SRC
148 plantation and the atmosphere – has been extensively described previously (Zona *et al.*, 2013).
149 Briefly, the EC system included a three-dimensional sonic anemometer (Model CSAT3,
150 Campbell Scientific, Logan, UT, USA) to measure the wind speed component fluctuations, and a
151 closed-path differential infrared gas analyzer (LI-7000, LI-COR, Lincoln, NE, USA) for the
152 measurements of the CO₂ and H₂O mole fractions in air. Both instruments sampled variables
153 continuously with a frequency of 10 Hz. The sonic anemometer and the inlets of the sampling
154 lines were situated at 5.8 m above the soil surface during a first period (from 1 June 2010 to 30
155 August 2011), and were raised to 6.6 m thereafter (from 31 August 2011 to 31 December 2013)
156 to match the rapid growth of the plantation. A vacuum pump positioned at the outlet of the LI-

157 7000 gas analyzer, generated a flow rate of about 20–22 l min⁻¹. This maintained a turbulent
158 flow regime in the sampling line – as required by standard EC methodology – to avoid
159 concentration dilution in the air samples between the sampling line inlet and the gas analyzer,
160 and the consequent, high-frequency fluctuation dampening (Munger *et al.*, 2012). To eliminate
161 the fluctuations caused by the pump two buffers (volume of 0.5 l each) were positioned between
162 the pump and the outlet of the analyzer. The sampling tubes were heated and thermally insulated
163 from the environment to prevent condensation and deliquescence of the air samples in the inlet
164 tubes. These phenomena can cause dampening of the water vapor high frequency fluctuations
165 possibly leading to large underestimates of the LE fluxes (Fratini *et al.*, 2012).

166 Several environmental variables were continuously recorded. Volumetric soil water content
167 (SWC) was measured horizontally in the soil layers 0–30 cm, 0–20 cm, 0–10 cm, and
168 horizontally at specific depths of 1 m, 60 cm, 40 cm, 30 cm, and 20 cm below the surface, using
169 moisture probes (TDR model CS616, Campbell Scientific, Logan, UT, USA). Soil temperature
170 was recorded by temperature probes which provided the average temperature of a soil layer of 8
171 cm depth (model TCAV-L averaging thermocouples, Campbell Scientific, Logan, UT, USA).
172 Soil heat flux (G) was measured by eight heat flux plates (HFT3, REBS Inc., Seattle, WA,
173 USA) installed at 6–8 cm depth. Air temperature and relative humidity were recorded on the EC
174 mast using a Vaisala probe (model HMP45C, Vaisala, Helsinki, Finland). The net radiation was
175 measured with a four-component radiometer (model CNR1, Kipp & Zonen, Delft, The
176 Netherlands) to give incoming (S) and reflected (S_r) solar (0.3–3 μm), and incoming (L_d) and
177 outgoing (L_u) longwave (far infrared 4.5–42 μm) radiation. Net radiation (R_n) was calculated
178 retrospectively using the equation:

$$179 R_n = (S - S_r) + (L_d - L_u) \quad (1)$$

180 Incoming photosynthetically active radiation (PAR; 400–700 nm) was recorded above the
181 canopy using quantum sensors (LI-190, LI-COR, Lincoln, NE, USA).

182

183 2.3 Gap-filling and post-processing

184 Fluxes of CO₂, LE, and H were calculated using the EdiRe software (R. Clement, University of
185 Edinburgh, UK; www.geos.ed.ac.uk/abs/research/micromet/EdiRe/) from high-frequency data
186 series divided in half-hourly averaging periods. The two-component rotation was applied to set
187 mean lateral and vertical wind velocity components to zero while the time delay between scalar

188 and vertical wind velocity fluctuations was determined by cross-correlation optimization (Foken
189 *et al.*, 2012). The frequency response correction was applied to the EC fluxes following Horst
190 (1997). The WPL H₂O vapor correction term of Webb *et al.* (1980) was applied to all the data
191 collected. A filter rejected data using the following criteria: (i) more than ten standard deviations
192 from the 30-minute mean for CO₂, and for the wind velocity components, u, v, and w; (ii) more
193 than one standard deviation for H₂O vapor; (iii) for quality flags 9 as suggested by Foken and
194 Wichura (1996) and Foken *et al.* (2004). To maximize the data coming from the plantation under
195 study only data with wind direction between 50° and 250° were used. In order to avoid the
196 possible underestimation of fluxes during stable (non-turbulent) conditions at night, data with
197 friction velocity (u*) below a threshold were treated separately using the procedure described by
198 Reichstein *et al.* (2005). The u* values adopted for each year were 0.15 m s⁻¹, 0.13 m s⁻¹, 0.18 m
199 s⁻¹ and 0.2 m s⁻¹ for the datasets of 2010, 2011, 2012 and 2013, respectively. A storage term –
200 about 3.4%, 3.8%, 3.1% and 3.7% of the cumulative NEE in 2010, 2011, 2012, and 2013,
201 respectively – was added to the CO₂ flux calculation before setting the u* thresholds. To follow
202 the rapid changes in canopy height, that characterized the SRC plantation, the displacement
203 height and the roughness length were calculated following the methodologies presented in Arya,
204 (1998) and Stull, (1988).

205 To estimate the 30-min values of ecosystem respiration (R_{eco}) and GPP, we used the Marginal
206 Distribution Sampling (MDS) method (Reichstein *et al.*, 2005) implemented in [www.bgc-](http://www.bgc-jena.mpg.de/~MDIwork/eddyproc/)
207 [jena.mpg.de/~MDIwork/eddyproc/](http://www.bgc-jena.mpg.de/~MDIwork/eddyproc/) (2013 version). This method was adopted by the FLUXNET
208 community as a standardized gap-filling and flux-partitioning technique (Moffat *et al.*, 2007;
209 Papale *et al.*, 2006). The fluxes of CO₂, H and LE were gap-filled to calculate the cumulative net
210 ecosystem production (NEP) and respective energy balance components with the error
211 propagated from the half-hourly averaged data into the annual uncertainties. To assess the
212 consistency of the EC measurements, we analyzed the linear regression between the half-hourly
213 sum of LE and H, measured by the EC system, versus the difference between R_n and G, obtained
214 with independent measurements. Heat storage in the biomass, in the air column below the EC
215 system and in the soil above the soil heat flux plates was not considered in this analysis.

216 To determine the relative contribution of the carbon exchange processes to the total exchange we
217 used the ratio GPP/R_{eco}. Values of GPP/R_{eco} less than unity indicate that the crop is a source of

218 carbon, while values of unity indicate the crop that is carbon-neutral ($NEE = 0$). When GPP
219 exceeds R_{eco} ($GPP/R_{eco} > 1$) the ecosystem is storing carbon (Falge *et al.*, 2002).
220 The energy partitioning and the impact of dry periods were evaluated using the evaporative
221 fraction (EF) approach. The instantaneous EF (dimensionless) was calculated from the LE and
222 the H fluxes values as follows:

$$EF_{\text{daytime}} = \frac{\int_{t_1}^{t_2} LE(t) dt}{\int_{t_1}^{t_2} [H(t) + LE(t)] dt} \quad (2)$$

224 where the time difference t_2-t_1 refers to the time from 11:00 to 14:00 (UTC + 1) in the present
225 study. The growing season was defined as the months with net carbon uptake.
226

227

228 2.4. Plant and leaf area index

229 Plant area index (PAI) was monitored in 96 plots (i.e., 12 genotypes x 2 former land-use types x
230 4 replicates), covering the double rows and the space between two adjacent double rows. PAI
231 was measured using the LAI-2000 and LAI-2200 Plant Canopy Analyzers (LI-COR, Lincoln,
232 NE, USA), by comparison of above- and below-canopy readings with a 45° view cap. These
233 indirect PAI measurements were taken from July to November in 2010, from April to November
234 in 2011, from June to November in 2012, and from March to November in 2013. In each plot
235 two diagonal transects were made between the rows, and along each transect measurements were
236 taken with the sensor parallel and perpendicular to the row. Leaf area index (LAI) was obtained
237 by subtracting the woody canopy area index (obtained during leafless periods) from the total
238 plant area index (Wilson *et al.*, 2000). LAI and PAI measurements of the plantation were
239 described and discussed in more detail by Broeckx *et al.* (2014).

240 To examine the role of LAI in controlling the GPP, and to minimize the confounding effects of
241 varying radiation levels, we analyzed GPP over a narrow range of incident PAR (GPP_{PAR} : GPP
242 when PAR was between 1000 and 1400 $\mu\text{mol m}^{-2} \text{s}^{-1}$) as a function of LAI for each growing
243 season. We also examined the relationships between LE and net radiation, air temperature, and
244 VPD, sorted by two levels of LAI (0-1 and > 4) and tested the influence of LAI using the
245 ANCOVA test.

246

247 2.5 Surface conductance

248 The surface conductance (G_s , mol m⁻² s⁻¹) was determined from the rewritten Penman-Monteith
 249 equation (Wohlfahrt *et al.*, 2009; Monteith and Unsworth 2013) as follows:

$$G_s = \frac{g_a \gamma}{(1 + \beta) + (\Delta + VPD c_p g_a / (P A)) - \Delta - \gamma} \quad (3)$$

250
 251 with g_a = aerodynamic conductance for heat and water vapor; γ = psychrometric constant; β =
 252 Bowen ratio (the ratio of sensible to latent heat flux, or H/LE); Δ = slope of the saturation water
 253 vapor pressure curve; VPD = vapor pressure deficit; c_p = specific heat of the air; P = atmospheric
 254 pressure; and A = available energy. The available energy was taken as being equal to H + LE,
 255 measured by eddy covariance, instead of the measured net radiation minus soil heat flux,
 256 throughout the whole study. Two main reasons justified this approach: (i) energy storage into the
 257 soil above the heat flux plate(s) as well as storage in the canopy (stem, branches and leaves) and
 258 in the air column below the measuring point, which may influence the specific half-hourly
 259 energy balance closure, were not quantified; (ii) forcing H and LE to be equal to net radiation
 260 minus soil heat flux and closing the energy balance according to the Bowen ratio, generally
 261 resulted in a significantly higher noise and unrealistic values of G_s . This Bowen ratio correction
 262 is no longer recommended as a universally applicable and a valid solution to a lack of energy
 263 balance closure, because there is empirical evidence that most of the missing energy should be
 264 assigned to H (Foken *et al.*, 2012).

265 The aerodynamic conductance (g_a , mol m⁻² s⁻¹) was calculated from direct measurements by the
 266 EC system according to Liu *et al.* (2007) as:

$$g_a = \frac{\phi_m u_*^2}{\phi_v u_z} + \frac{6.266}{u_*^{-2/3}} \quad (4)$$

267
 268 where ϕ_m and ϕ_v = stability functions for momentum and water vapor transfer; u_* = friction
 269 velocity; u_z = wind speed at the reference height z. The righthand side of Eq. (4) expresses the
 270 empirically derived excess resistance for scalars relative to momentum (Thom, 1972).

271 The universal stability functions were applied following Dyer (1970) as:

$$\phi_v = \phi_m^2 = \left(1 - 16 \frac{z - d}{L}\right)^{-1/2} \quad (5)$$

272 for unstable conditions and as:

$$\phi_v = \phi_v = 1 + 5.2 \frac{z - d}{L} \quad (6)$$

273 for stable conditions, where d = zero plane displacement, and L = the Obukhov length.

274 The conversion of g_a from m s^{-1} into $\text{mol m}^{-2} \text{s}^{-1}$ was made using the combined Boyle's and
275 Charles's gas laws (Monteith and Unsworth, 2013).

276 An estimate of mean stomatal conductance was made following:

$$g_s = G_c / LAI \quad (7)$$

277 where G_c is the canopy conductance (Lindroth, 1993). Since we did not measure soil and
278 understory LE separately, we assumed that $G_c = G_s$ when the canopy is dry and for $LAI > 3$
279 (Herbst, 1995). During these conditions soil and understory LE can be considered as the minor
280 component of LE, although they cannot be completely neglected (Lindroth, 1993).

281 The physiological control of LE, as compared to the climatological control, was estimated using
282 the Penman-Monteith equation rewritten according to Jarvis and McNaughton (1986):

$$\Omega = \frac{1 + \Delta/\gamma}{1 + \Delta/\gamma + g_a/G_s} \quad (8)$$

283 where Ω = decoupling factor ($0 < \Omega < 1$). A value of Ω close to one indicates that LE is mainly
284 controlled by the available energy; a change of G_c results in a very small change of LE (i.e. a de-
285 coupled system dominated by climatological control). In contrast, a small Ω value (close to 0)
286 indicates that LE is mainly controlled by VPD and G_c (i.e. a well-coupled system with a
287 physiological control dominating). In our study we chose the equilibrium LE as the reference
288 representing the evaporation from a wet surface without any advective influences. The ratio
289 between LE and its equilibrium rate can be described in the following form:

$$\alpha = LE / \frac{\Delta A}{\Delta + \gamma} \quad (9)$$

290 where α is the so-called Priestley-Taylor coefficient (Priestley and Taylor, 1972). The deviation
291 of α from unity suggests either well watered conditions with LE enhanced by advective
292 processes ($\alpha > 1$) or water-limited ($\alpha < 1$) conditions.

293 The half-hourly values of G_s , Ω , and α were eliminated only for conditions with dry canopy and
294 integrated into daily means weighted by R_n (Wilson *et al.*, 2000). The canopy was considered as
295 dry when the amount of intercepted water from precipitation or potential dew condensation was

296 exceeded by the cumulative equilibrium evaporation. Therefore the interception capacity (mm)
297 was considered to be equal to 0.2 of LAI (Iritz *et al.*, 2001).

298

299 3. Results

300 3.1. Meteorological conditions and LAI development

301 The evolution of the mean daily SWC (in %) along with the water table depth is shown in Fig. 1
302 panel A: SWC followed the variations in water table depth throughout the entire duration of the
303 study. Precipitation (Fig. 1, panel B) was 556 mm in 2010 (only from June to December), versus
304 718 mm in 2011, 857 mm in 2012 and 947 in 2013 (entire years), respectively. Precipitation
305 during the period June – September was 355 mm in 2010, 334 mm in 2011, 299 mm in 2012 and
306 407 in 2013. The average daily air temperature (Fig. 1, panel B) during the period June -
307 September ranged between 18°C and 22°C in all four years. The seasonal dynamics of the daily
308 average R_n were similar in all four years (Fig 1, Panel C).

309 Although the environmental conditions were rather similar during the four years of the study, the
310 LAI development (Fig. 1, panel D) showed a remarkable difference between the first rotation
311 (2010 and 2011) and the second rotation (2012 and 2013). During the first rotation LAI reached
312 values from 0.96 (± 0.4) in August 2010 to 2.0 (± 1.2) in October 2011. During the second
313 rotation the multiple-stem coppice culture reached values of 5.1 (± 1.5) in September 2012 and
314 4.5 (± 0.84) in August 2013.

315

316 3.2. Temporal dynamics of CO₂ and ET fluxes

317 The net carbon balance during the first rotation was 75.2 (± 4.4) g C m⁻² in 2010 (from June to
318 December), and -95.6 (± 5.9) g C m⁻² in 2011. After the harvest (second rotation) the net carbon
319 balance was 151.0 (± 10.5) g C m⁻² in 2012 and -274.6 (± 18.8) g C m⁻² in 2013. Considering the
320 two two-year rotations of the SRC plantation together the overall carbon balance was -144.0 (\pm
321 22.8) g C m⁻². The average rate of carbon uptake during the growing season was -39.6 (± 16.4) g
322 C m⁻² per month during the first rotation and -59.6 (± 42.5) g C m⁻² per month during the second
323 rotation. The plantation was also characterized by a different length of the growing season within
324 the same rotation. In 2010 and 2011 (i.e., first rotation) the growing season was from August to
325 September, and from April to September respectively. In 2012 and 2013 (i.e., the second
326 rotation) the growing season was from June to August 2012, and from April to October 2013,

327 respectively (Fig. 2). The vegetation started later in the first year of each rotation because the
328 crop had to get started either from the woody cutting (first rotation) or from the harvested stem
329 (second rotation).

330 The GPP/R_{eco} ratio exceeded 1 during the months with a net carbon uptake: considering the two
331 rotations together GPP/R_{eco} exceeded 1 from May to September, and ranged from 1.3 (± 0.36) in
332 May to 1.7 (± 1.0) in July (Fig. 3). Annual GPP/R_{eco} values were 0.88 in 2010, 1.07 in 2011, 0.91
333 in 2012 and 1.35 in 2013.

334 The cumulative ET measured during the first rotation was 241.7 mm and 349.9 mm for 2010
335 and 2011, respectively, while during the second rotation, ET was 464.6 mm and 372.1 mm for
336 2012 and 2013, respectively. During the 2010 growing season ET increased gradually from 1.7
337 (± 0.47) mm d^{-1} in mid-June to 3.42 (± 1.1) mm d^{-1} in mid-July following the rapid canopy
338 development. In the following year (2011) the rapid increase of ET from 0.33 (± 0.2) mm d^{-1}
339 observed at the beginning of March 2011 to 2.1 (± 1.0) mm d^{-1} at the end of June 2011 was
340 consistent with the rapid increase of the available R_n and with the increasing LAI from 0.62 (\pm
341 0.3) in March 2011 to 1.33 (± 0.7) in June 2011. A similar pattern was observed in 2012, and in
342 2013, i.e., during the second rotation. The difference in length of the active growing season was
343 mainly determined by differences in the LAI initiation: e.g., in 2013, the plantation reached an
344 LAI of 2.4 on DOY 151, while in 2012 a similar LAI was reached only on DOY 189. Due to the
345 larger LAI (after coppicing as compared to the two years before coppicing) the growing season
346 ET was constantly higher compared to the previous years before the coppicing (Fig. 4, panel A).
347 Unlike the other growing seasons, in 2012 the plantation was coppiced during the previous
348 winter (in February 2012); this affected the microclimate at the plantation. Throughout the entire
349 spring of 2012 there was only bare soil with stumps covered by the debris of branches and
350 woody chips left after the harvest. As a result, ET was mainly dominated by soil evaporation
351 with lower values measured in March and April 2012 (i.e., 14.1 and 33.2 mm per month) as
352 compared to the same period in 2011 (values of 21.8 and 53.1 mm per month in March and
353 April, respectively; Table 2). In May 2012 the stumps started to resprout, characterized by a very
354 fast growth rate of the stems (with an average of ~ 10 shoots per coppiced stool) and of the LAI.
355 A consistent observation in each year was the rapid decline in ET related to the canopy
356 senescence starting in September till the end of the season. The overall closure of the surface
357 energy balance was on average 0.68. More specifically, for the 2010 growing season, it was 0.71,

358 while for the other three growing seasons it ranged from 0.67 in 2011 and 2013 to 0.70 in 2012.
359 The temporal variation of the energy balance closure indicated a higher energy balance closure in
360 the middle of the growing season as compared to the winter periods (Fig. 4, panel C). The lack of
361 energy balance closure may indicate that the absolute values of ET were slightly underestimated.
362 The temporal dynamics of the EF showed a clear seasonality in the energy partitioning (Fig. 4,
363 panel B). The conversion of available energy was favoring LE in spring, summer and autumn,
364 while during winter most of the available energy was partitioned into H.
365 The maximum EF between 0.8 and 1 coincided with the maximum LAI and indicated that most
366 of the available energy was converted into LE at that time. In May–July 2011 and in June–July
367 2013, we observed a consistent reduction of the EF, i.e., an increase of H and of the Bowen ratio.
368 This reduction was most probably caused by the lowering of the SWC. The EF did not show a
369 relevant diurnal trend: median values ranged from 0.6 to 0.72 from 09:00 to 17:00 (UTC + 1)
370 (Fig. 5). The magnitude of the EF indicates that the plantation did not suffer from severe, or
371 prolonged, periods of drought during the growing season (with the exception of the short periods
372 of May–June 2011, and of June 2013).

373

374 3.3 Role of LAI in controlling GPP, LE, and G_s

375 The relationships between LE and net radiation, air temperature and VPD at different values of
376 LAI are presented in Fig. 6. The analysis of covariance (ANCOVA) revealed a significant effect
377 of LAI on LE, after removing for the effect of net radiation, $F(1,1246) = 249.3$, $p < 0.05$, as well
378 as after removing for the effect of air temperature $F(1,1246) = 5.79$, $p < 0.05$, and VPD
379 $F(1,744) = 82.8$, $p < 0.05$. Statistical parameters of the regressions shown in Fig. 6 are
380 summarized in Table 1. Beside the significantly different slopes, the coefficient of determination
381 of the relationships between LE versus net radiation, air temperature and VPD was always higher
382 for the values with $LAI > 4$ as compared to values with LAI between 0 and 1. This indicated that
383 LE from the well-developed canopy was generally not only higher, but also less variable in
384 relation to climatological variables as compared to the LE from the sparse canopy which was
385 dominated by the soil and understory LE.

386 The temporal variation of G_s , α , and Ω showed pronounced seasonal patterns (Fig. 7). As
387 expected these three bulk parameters were positively and significantly correlated (Fig. 8). The
388 increase of LAI was accompanied by an increase in G_s . Nevertheless, there were some occasions

389 when G_s declined despite an increasing LAI; these were associated with short periods of drought.
390 This was most pronounced in May 2011 when LAI development was significantly inhibited.
391 During the periods with low LAI, G_s was mainly driven by (i) soil evaporation which was
392 strongly dependent on surface soil moisture and thus on the distribution and the magnitude of
393 precipitation (Figs. 1 and 7); and (ii) understory transpiration dependent on the density and the
394 species composition of the weed vegetation, its phenology and physiological activity. The
395 average values of G_s were $0.35 \text{ mol m}^{-2} \text{ s}^{-1}$ and $0.24 \text{ mol m}^{-2} \text{ s}^{-1}$ for the foliated and the
396 unfoliated periods, respectively. The mean Ω was 0.35 and 0.23, and the mean α was 0.77 and
397 0.53 for the foliated and the unfoliated periods, respectively.

398 The relationship between the GPP_{PAR} and LAI was well described by a three-parameter
399 exponential function (Fig. 8, panel A). Until LAI reached 2 the relationship appeared to be nearly
400 linear with a mean slope of $8.8 \mu\text{mol m}^{-2} \text{ s}^{-1}$ per unit of LAI. For larger LAI values the
401 relationship asymptotically approached the maximum around $30 \mu\text{mol m}^{-2} \text{ s}^{-1}$. The intercept of
402 GPP_{PAR} (equal to $5 \mu\text{mol m}^{-2} \text{ s}^{-1}$) suggests the contribution of weeds to the CO_2 uptake. In
403 contrast to GPP, surface conductance showed a much weaker relationship with LAI (Fig. 6,
404 panel B). In addition, this relationship showed a less asymptotic behavior which may indicate a
405 slight reduction of the water use efficiency when LAI reached the inflection point of the GPP vs.
406 LAI relationship, which was close to an LAI of 2. Similar non-linear relations were found for α
407 and Ω (Fig. 6, panels C and D, respectively). The mean slope of the relationship between G_s and
408 LAI (Fig. 8, panel B) suggests that an increase of LAI by $1 \text{ m}^2 \text{ m}^{-2}$ caused an increase of G_s by
409 $0.043 \text{ mol m}^{-2} \text{ s}^{-1}$. However, the first half of this increase is determined by the mean slope of
410 $0.061 \text{ mol m}^{-2} \text{ s}^{-1}$ and is reached at an LAI of 2.2. The second half of this increase is
411 characterized by a less steep slope of $0.029 \text{ mol m}^{-2} \text{ s}^{-1}$. In the case of α , the mean slope was 0.09
412 per $1 \text{ m}^2 \text{ m}^{-2}$ of LAI with a slightly more pronounced asymptotic limit for higher LAI values. The
413 first half of the α versus LAI relationship was reached at an LAI of 2.1 and was characterized by
414 a slope of 0.14, while the second half was characterized by a slope of 0.05 only. The non-linear,
415 positive relationship between Ω and LAI was described by a mean slope of 0.028. The first half
416 of this increase reached before LAI of 2.1 was characterized by a slope of 0.045, and the second
417 half by a slightly less steep increase of 0.017 per $1 \text{ m}^2 \text{ m}^{-2}$. When related to LAI all of the four
418 investigated variables (GPP_{PAR} , G_s , Ω and α) showed a departure from the main trend during the
419 drought episodes in May-June 2011 and in June 2013 (Fig. 9).

420 Light saturated (incident solar radiation $> 500 \text{ W m}^{-2}$) g_s , estimated from the EC measurements,
421 showed a strong negative relationship with VPD; this relationship was well described by an
422 exponential decay function $g_s = g_{sref} - m \ln VPD$ (Oren et al., 1999) (Fig. 10, panel A). The
423 reference stomatal conductance (g_{sref}) is the g_s at a VPD of 1 kPa and is represented by the
424 intercept of this function, i.e., $0.12 \text{ mol m}^{-2} \text{ s}^{-1}$. The parameter m representing the so-called
425 stomatal sensitivity was equal to $0.055 \text{ mol m}^{-2} \text{ s}^{-1} \ln(\text{kPa})^{-1}$. The ratio between m and g_{sref}
426 provides an empirical hydraulic conductivity parameter, and was equal to $0.45 \ln(\text{kPa})^{-1}$. Values
427 of g_s close to the maximum g_s occurred during conditions of high relative humidity.
428 Measurements during such periods are inherently prone to errors in the EC water vapor flux
429 measurements and to errors in the measurements of VPD itself (by capacitance hygrometers).
430 We therefore excluded the values with a VPD below 0.75 kPa and obtained slightly different
431 parameters: $g_{sref} = 0.13 \text{ mol m}^{-2} \text{ s}^{-1}$, $m = 0.0629 \text{ mol m}^{-2} \text{ s}^{-1} \ln(\text{kPa})^{-1}$ and the ratio $m/g_{sref} = 0.49$
432 $\ln(\text{kPa})^{-1}$. In the narrow range of VPD between 0.9 and 1.1 kPa (around the reference g_s) g_s
433 showed a significant linear relation with incident solar radiation where the g_s increased by 0.014
434 $\text{mol m}^{-2} \text{ s}^{-1}$ for every 100 W m^{-2} of incident solar radiation (Fig. 10, panel B).

435

436 4. Discussion

437 Although SRC plantations are managed in a similar way to agricultural crops (e.g., soil
438 preparation, weed control, irrigation, fertilization, etc.) the magnitude and the temporal dynamics
439 of their GPP/ R_{eco} are comparable to those of deciduous forests (Fig. 3). In unmanaged
440 ecosystems the balance between respiratory and assimilatory processes is affected by climate
441 change (Houghton *et al.*, 1996). Systematic changes in the length of the growing season
442 (Randerson *et al.*, 1999; Keyser *et al.*, 2000) indicate an extension of the period favorable for
443 assimilation. In an intensively managed crop –as the SRC of this study – the impact of the
444 management on the length of the growing season appears to be more important; as highlighted
445 by the change in length of the growing season after the biomass was harvested (i.e., second
446 rotation; Fig. 2). The LAI values observed in the present study fell within the range of 4–12 for
447 well-established SRC plantations of poplar or willow (Lindroth *et al.*, 1994; Ceulemans *et al.*,
448 1996; Liberloo *et al.*, 2006; Petzold *et al.*, 2010, Fischer *et al.*, 2013). The development of LAI –
449 and of canopy closure – depends on plant density, genotypic variety, and vitality of the crop; all
450 these depend on the management regime. The high spatial variability of mean canopy LAI

451 observed was due to the significant genotypic differences in LAI while the difference between
452 the first and second rotation was due to the multiple stems present after the harvest. This spatial
453 heterogeneity of LAI was most probably also responsible for the unexpected increase of
454 aerodynamic roughness with LAI within the particular growing seasons. Similar dynamics of
455 LAI development, with a peak in the last part of the summer, have previously been described for
456 poplar and willow (Lindroth *et al.*, 1994; Ceulemans *et al.*, 1996; Guidi *et al.*, 2008, Fischer *et*
457 *al.*, 2013).

458 LAI development is inherently related to the partitioning of the available energy, to ET and to
459 the GPP dynamics (Iritz and Lindroth, 1996; Wilson *et al.*, 2000, Blanken *et al.*, 2001, Fischer *et*
460 *al.*, 2013). The cumulative ET measured during the first year was similar to that reported by
461 Fischer *et al.* (2013): a value of 259.4 mm yr⁻¹ (from the same period of July to December as in
462 our study). In the following years our cumulative ET values were slightly lower as compared to
463 the values reported by Fisher *et al.* (2013) (i.e., 549.2 mm yr⁻¹ and 606.6 mm yr⁻¹, respectively).
464 For a *P. tremula* plantation in Germany an ET value of 441 mm yr⁻¹ has been reported (Lasch *et*
465 *al.*, 2010), similar to the value of 403 mm yr⁻¹ for a *P. tremuloides* plantation in Canada (Black *et*
466 *al.*, 1996). A number of modeling and experimental studies carried out in various countries
467 across Europe have pointed out that the water use by SRC is substantially higher than that of
468 traditional agricultural crops or grasslands (Hall *et al.*, 1996, 1998; Allen *et al.*, 1998; Perry *et*
469 *al.*, 2001; Petzold *et al.*, 2010). At our site the highest ET rates of *ca.* 5 mm d⁻¹ were typically
470 recorded during the late spring and summer, i.e., the periods with the highest evaporative
471 demand. If ET is not limited by undeveloped LAI, this coincidence of maximum ET with the
472 highest evaporative demand generally indicates an adequate water supply. These results are
473 similar to peak values of daily ET in July-August (5 to 6 mm d⁻¹) during the second year after
474 coppice at a poplar plantation in central Europe (Fischer *et al.*, 2013) and lower than the peak ET
475 values of 8 to 10 mm d⁻¹ for poplar SRC in the warmer climatic conditions of Italy (Tricker *et*
476 *al.*, 2009). These two last studies were conducted on monoclonal plantations of *Populus nigra* ×
477 *P. maximowiczii* (clone J-105) respectively *Populus x euramericana* (clone I-214), while our site
478 was a multi-genotype plantation characterized by significant genotypic differences in terms of
479 biomass production and LAI (Broeckx *et al.*, 2012; Verlinden *et al.*, 2013).

480 The energy balance closure of 0.7 to 0.83 reported here is typical of that observed in many
481 experiments across international EC networks (Wilson *et al.*, 2002a). A more pronounced lack of

482 energy balance closure in winter is most probably caused by an underestimation of the measured
483 LE due to signal attenuation (Fratini *et al.*, 2012). It is quite common practice to distribute this
484 residual energy to H and LE according to the Bowen ratio (Shuttleworth, 2007). However, this
485 procedure was later recognized as not generally valid (Foken, 2008). Some studies indicate that
486 the lack of energy balance closure is associated mainly with H transported by large eddies not
487 detectable by the EC method (Mauder and Foken, 2006; Foken, 2008; Ingwersen *et al.*, 2011). It
488 is therefore difficult to quantify the final error in our ET measurements due to energy balance
489 closure.

490 EF is related to the partitioning of the available energy (Crago and Brutsaert, 1996) and has been
491 used as an index of drought (San Miguel-Ayanz *et al.*, 2000; Heim, 2002 Schwalm *et al.*, 2010).
492 As indicated by the trend and the magnitude of the EF during the growing season we did not
493 observe prolonged periods of drought apart from the two short episodes in May-June 2011 and in
494 June 2013. In a recent meta-analysis to quantify the drought effects on the carbon cycle and on
495 the terrestrial carbon sink (Schwalm *et al.*, 2010) a critical value of 0.4 was reported at the time
496 of the heatwave that occurred across Europe in 2003. During the physiologically active periods,
497 the EF in our study averaged 0.65 (± 0.065) and approached or slightly decreased below the
498 critical 0.4 threshold in the late spring drought period of May 2011 and also slightly in June
499 2013. The diurnal trend of EF showed nearly constant values with only a slight increase toward
500 the late afternoon; this agreed with the daytime self-preservation of the EF assumption (Sugita
501 and Brutsaert, 1991; Brutsaert and Sugita, 1992; Crago and Brutsaert, 1996). However, more
502 recent analyses (Peng *et al.*, 2013; Gentine *et al.*, 2011) indicated a consistent daytime trend of
503 the EF.

504 The relations between g_s , G_c , G_s and VPD and solar radiation, water availability and temperature
505 have been the core of various ecophysiological models (Lindroth *et al.*, 1994; Cienciala and
506 Lindroth, 1995; Hall *et al.*, 1996; Kim *et al.*, 2008). Since G_c is a product of g_s and LAI, G_c is
507 tightly correlated with LAI or more specifically with its solar equivalent (Čermák, 1989, Kim *et al.*
508 *et al.*, 2008). In the case of G_s , the relationship is hampered by the influence of soil and understory
509 LE. In spite of this soil and understory LE we found a significant relation between G_s and LAI
510 with a mean slope of $0.043 \text{ mol m}^{-2} \text{ s}^{-1}$, which is consistent with other studies. For instance,
511 Wilson *et al.* (2000) reported the slope of the relationship of g_s versus LAI as $0.63 \text{ mol m}^{-2} \text{ s}^{-1}$ for
512 a mixed deciduous forest, while for an aspen forest with a hazelnut understory a value of 0.048

513 mol m⁻² s⁻¹ has been reported (Blanken *et al.*, 2004). In general, the positive correlation between
514 g_s and LAI is the highest when the soil surface is dry, but there is adequate water available
515 deeper in the root zone. However, under the Belgian climate conditions with a relatively high
516 annual precipitation well distributed over the season, there are hardly any conditions of a dry soil
517 surface over a long period of time.

518 The average G_s of 0.35 mol m⁻² s⁻¹ during the foliated period in this study is comparable to the
519 average G_s of 0.27 mol m⁻² s⁻¹ for a monoclonal poplar plantation (*Populus nigra* x *P.*
520 *maximowiczii*) in the Czech Republic over several growing seasons including one year after
521 coppice with a very low ET (Fischer *et al.*, 2012). In an SRC of willow in Sweden G_c values
522 ranged from 0.45 to 1.1 mol m⁻² s⁻¹ (Lindroth, 1993) and these values slightly differed from the
523 maximum G_s of our study that reached 0.76 mol m⁻² s⁻¹ in September 2012. In an attempt to
524 quantify the partitioning of LE and H during the warm season (mid-June to late August) at 27
525 FLUXNET sites covering a wide range of terrestrial ecosystems, Wilson (2002b) reported a
526 range of G_s values at midday that varied from 0.4 to 0.67 mol m⁻² s⁻¹ for deciduous forests while
527 it was 0.66 mol m⁻² s⁻¹ for a conventional poplar plantation. By comparing our mean G_s of 0.35
528 mol m⁻² s⁻¹ with the G_s 0.64 mol m⁻² s⁻¹ of the hypothetical reference grass (Allen *et al.*, 1998) we
529 can infer that water consumption of our poplar SRC was significantly lower than that to be
530 expected from the reference grass, despite the higher aerodynamic conductance of the
531 aerodynamically rougher SRC.

532 The average Ω equal to 0.35 indicated a rather good coupling to the atmosphere. This value
533 mathematically means that changing G_s by 10% results in a 6.5% change in LE; thus stomata
534 play an important role in controlling LE. Interestingly, we did not observe a decrease of g_a or
535 u/u_{*} (data not shown) with an increase of LAI suggesting that this multi-genotype SRC was
536 aerodynamically smoother during the unfoliated periods. This also means that the positive linear
537 relationship between LAI and Ω was mainly due to the significant increase of G_s.

538 The average value of Ω is consistent with many other studies focusing on poplar or willow SRC:
539 similar results were obtained for a willow stand in southern Sweden with an Ω value of 0.4
540 (Cienciala, 1994). For a poplar SRC a decoupling coefficient between 0.16 and 0.6 – with an
541 average of 0.41 – was reported and the highest values were associated with the higher LAI
542 values (Fischer *et al.* 2012). Likewise, Lindroth (1993) found that the decoupling coefficient was
543 low (0–0.4) at LAI < 1; afterwards, with increasing LAI, the Ω value increased into the range of

544 0.6 to 0.8. So, their SRC stand (Lindroth, 1993) was well-coupled to the atmosphere for low
545 values of LAI, and it was practically de-coupled for LAI values above about two. An average Ω
546 of 0.66 was reported for a high-density plantation of hybrid poplars (*P. trichocarpa* x *P.*
547 *deltoides*) in the Pacific Northwest (Hinckley *et al.*, 1994), which also means a poor coupling to
548 the atmosphere. In contrast, a rather low decoupling coefficient of 0.31 was reported for a boreal
549 aspen (*P. tremuloides*) forest in Canada (Blanken *et al.*, 1997). Likewise, values of the
550 decoupling coefficient never exceeded 0.3 for *P. euphratica* grown in a plantation on degraded
551 cropland with increased salinity in Uzbekistan (Khamzina *et al.*, 2009).

552 The mean annual Priestley-Taylor coefficient, α , equal to 0.77 is very similar to the α value of
553 0.7 reported for a deciduous mixed forest (Wilson *et al.*, 2000) and slightly lower than a
554 Canadian aspen forest with α of 0.99 (Blanken *et al.*, 2004). The average α value of 0.77 also
555 means that the ET of the poplar SRC was 23% lower than the equilibrium ET. This equilibrium
556 is in addition on average 8% lower than the ET of the hypothetical reference grass cover without
557 water and nutrient limitations (Allen *et al.*, 1998). This implies that ET of our multi-genotype
558 SRC was, in general, significantly lower than ET of the grasslands confirming the recent findings
559 reported by Fischer *et al.* (2013).

560 The analysis of the stomatal conductance showed a significant decrease of g_s in response to VPD
561 and an increase in response to solar radiation: these relationships reflect the well-known fact that
562 plants open their stomata when exposed to light and close them when the evaporative demand of
563 the atmosphere is increasing (Lindroth *et al.*, 1993; Kim *et al.*, 2008). By doing so plants
564 maximize the carbon uptake while they prevent the decrease of the leaf turgor and xylem
565 cavitation and embolism (Domec *et al.*, 2012).

566 The ratio of m to g_{sref} represents an important hydraulic parameter and indicates whether a
567 particular species is able to maintain a constant minimum leaf water potential (isohydric) via its
568 stomata or has a lower control of its leaf water potential (anisohydric). (Domec *et al.*, 2012).

569 Poplar is known to exhibit the two contrasting hydraulic behaviors (Domec *et al.*, 2012;
570 Hinckley *et al.*, 1994). The ratio of m to g_{sref} equal to $0.45 \text{ mol m}^{-2} \text{ s}^{-1} \ln(\text{kPa})^{-1}$ found in the
571 present study indicates a rather weak stomatal control as compared to a generic value of 0.6 mol
572 $\text{m}^{-2} \text{ s}^{-1} \ln(\text{kPa}^{-1})$ for isohydric species (Oren *et al.*, 1999). Mean leaf-level ratios of m and g_{sref}
573 equal to $0.45 \text{ mol m}^{-2} \text{ s}^{-1} \ln(\text{kPa})^{-1}$ based on porometric measurements, and of $0.64 \text{ mol m}^{-2} \text{ s}^{-1}$
574 $\ln(\text{kPa})^{-1}$ based on the sap flow technique, were previously reported for hybrid poplar (*P.*

575 *trichocarpa* × *P. deltoides*) by Kim *et al.* (2008). A typical isohydric behavior with mean ratio of
576 m to g_{sref} around $0.62 \text{ mol m}^{-2} \text{ s}^{-1} \ln(\text{kPa})^{-1}$ was reported for a mature poplar hybrid (*P. nigra* ×
577 *P. maximowiczii*) stand in Germany (Schmidt-Walter *et al.*, 2014). The rather lower stomatal
578 control of our multi-genotype SRC is in accordance with previous studies suggesting that this
579 SRC potentially had a higher sensitivity to prolonged drought spells and exhibited a different
580 strategy characterized by leaf abscission rather than by a tight stomatal control (Pita *et al.*, 2013).
581 This rather anisohydric behavior may put our multi-genotypic poplar SRC at greater risk of
582 xylem dysfunction in extreme environmental conditions compared to SRC with species
583 characterized by a purely isohydric behavior as e.g., the monoclonal SRC (*P. nigra* × *P.*
584 *maximowiczii*) presented by Schmidt-Walter *et al.* (2014).
585 The g_s of $0.13 \text{ mol m}^{-2} \text{ s}^{-1}$ under reference meteorological conditions (VPD of $1 \pm 0.1 \text{ kPa}$ and
586 incident solar radiation $> 500 \text{ W m}^{-2}$) observed in the present study was lower than the g_{sref} close
587 to $0.45 \text{ mol m}^{-2} \text{ s}^{-1}$ reported for a hybrid poplar plantation (*P. x canadensis*) in northern Italy
588 (Migliavacca *et al.*, 2009). This might be partly explained by differences in LAI. The maximum
589 LAI in the study of Migliavacca *et al.* (2009) was only 2, and thus a relatively larger portion of
590 the canopy was exposed to the incident solar radiation as compared to the maximum LAI values
591 of 3 to 5 observed in the present study. At the same time soil and understory LE still significantly
592 influenced G_s for an LAI of 2, and from that inferred g_s . In contrast, Kim *et al.* (2008) found g_{sref}
593 values within the range of 0.070 to $0.142 \text{ mol m}^{-2} \text{ s}^{-1}$ measured by sap flow and porometer
594 techniques, values that are more consistent with our findings.

595 Summarizing the relationships presented and discussed, g_s was an important variable that is
596 physiologically related to transpiration and to GPP. The diurnal variation of g_s can be well
597 predicted using the physically based relationships between incident solar radiation and VPD.

598

599 5. Conclusion

600 The SRC plantation examined in this study became a carbon sink at the end of the second
601 rotation. Despite the intensive management, the magnitude and the annual temporal dynamics of
602 the SRC, the GPP/R_{eco} ratio appears to be similar to a deciduous forest. The ET was significantly
603 lower than the equilibrium evaporation and lower than the ET of a hypothetical reference crop;
604 this observation disputes the general perceptions of poplar SRC to be big water consumers. The
605 magnitude and the rapid development of LAI, characteristic for an SRC, was apart from the

606 meteorological conditions, the main biophysical driver of the seasonal and intra-seasonal
607 variation in carbon uptake and in evapotranspiration. Therefore, we suggest that the GPP_{PAR} and
608 G_s (or alternatively α) could be used as indicators of the carbon uptake and the ET of poplar SRC
609 without water stress wherever the LAI and the common meteorological variables are available.
610 Longer observations should evaluate the full impact of the management and should give more
611 reliable assessments of the water and carbon balances.

612

613

614

615

616

617

618

619

620

621

622

623

624

625

626

627

628

629

630

631

632

633

634

635

636

637 Acknowledgments

638 This research has received funding from the European Research Council under the European
639 Commission's Seventh Framework Programme (FP7/2007-2013) as ERC grant agreement n°.
640 233366 (POPFULL), as well as from the Flemish Hercules Foundation as Infrastructure contract
641 ZW09-06. Further funding was provided by the Flemish Methusalem Programme and by the
642 Global Change Research Center AS CR (Brno, Czech Republic) as projects n°. LH12037 and n°.
643 CZ.1.07/2.3.00/30.0056. We gratefully acknowledge the excellent technical support of Joris
644 Cools and Jan Segers as well as the logistic support of Kristof Mouton at the field site.

645

646

647

648

649

650 References

651

652 AEBIOM, 2012. European Bioenergy Outlook. European Biomass Association, Statistical
653 Report, Brussels, November 2012, 123 pp. <http://www.aebiom.org>

654

655 Allen, R.G., Pereira, L.S., Raes, D., Smith, M. 1998. Crop evapotranspiration. In: Guidelines
656 for Computing Crop Water Requirements. FAO Irrigation and Drainage Paper No. 56, pp. 290.

657

658 Arya, S.P., 1998. Introduction to Micrometeorology. San Diego Academic Press, Inc., New
659 York, 303 pp

660

661 Aylott, M.C., Casella, E., Tubby, I., Street, N.R., Smith, P., Taylor, G., 2008. Yield and spatial
662 supply of bioenergy poplar and willow short-rotation coppice in the UK. *New Phytol.*, 178, 358-
663 370.

664

665 Baldocchi, D.D., 1997. Measuring and modelling carbon dioxide and water vapour exchange
666 over a temperate broad-leaved forest during the 1995 summer drought. *Plant, Cell and Environ.*,
667 20, 1108-1122.

668

669 Black, T. A., Hartog, G. D., Neumann, H. H., Blanken, P. D., Yang, P. C., Russell, C., & Novak,
670 M. D. 1996. Annual cycles of water vapour and carbon dioxide fluxes in and above a boreal
671 aspen forest. *Global Change Biology*, 2(3), 219-229.

672

673 Blanken, P.D., Black, T.A., Zang, P.C., Den Hartog, G., Neumann. H.H., Nesic. Z., Staebler. R.,
674 Novak. M.D., Lee, X., 1997. Energy balance and canopy conductance of boreal aspen forest:
675 partitioning overstory and understory components. *Journal. Geophys. Research.* 102, 28915-
676 28927.

677

678 Blanken, P.D., Black, T.A., 2004. The canopy conductance of a boreal aspen forest, Prince
679 Albert National Park, Canada. *Hydrol. Processes*, 18, 1561-1578.

680

681 Blanken, P.B., Black, T.A., Neumann, H.H., Den Hartog, G., Yang, P.C., Nesic, Z., Lee, X.,
682 2001. The seasonal water and energy exchange above and within a boreal aspen forest. *J.*
683 *Hydrol.*, 245, 118-136.

684

685 Brutsaert, W., Sugita, M., 1992. Application of self-preservation in the diurnal evolution of the
686 surface energy budget to determine daily evaporation, *J. Geophys. Res. D: Atmos.*, 97: 18377-
687 18382.

688

689 Broeckx, L.S., Verlinden, M.S., Ceulemans, R., 2012. Establishment and two-year growth of a
690 bio-energy plantation with fast-growing *Populus* trees in Flanders (Belgium): effects of genotype
691 and former land use. *Biomass Bioener.*, 42, 151-163.

692

693 Broeckx, L., Verlinden, M.S., Berhongaray, G., Zona, D., Fichot, S., Ceulemans, R., 2014. The
694 effect of a dry spring on seasonal carbon allocation and vegetation dynamics in a poplar
695 bioenergy plantation. *GCB Bioenergy*, 6, 473-487.
696

697 Calfapietra, C., Gielen, B., Sabatti, M., De Angelis, P., Miglietta, F., Scarascia-Mugnozza,
698 G., Ceulemans, R., 2003. Do above-ground growth dynamics of poplar change with time under
699 CO₂ enrichment? *New Phytol.*, 160, 305-318.
700

701 Calfapietra, C., Tulva, I., Eensalu, E., Perez, M., De Angelis, P., Scarascia-Mugnozza, G., Kull,
702 O., 2005. Canopy profiles of photosynthetic parameters under elevated CO₂ and N fertilization in
703 a poplar plantation. *Environ. Pollut.*, 137, 525-535.
704

705 Carrara, A., Janssens, I.A., Curiel Yuste, J., Ceulemans, R., 2004. Seasonal changes in
706 photosynthesis, respiration and NEE of a mixed temperate forest. *Agric. For. Meteorol.*, 126, 15-
707 31.
708

709 Ceulemans, R., Shao, B.Y., Jiang, X.N., Kalina, J., 1996. First- and second-year aboveground
710 growth and productivity of two *Populus* hybrids grown at ambient and elevated CO₂. *Tree*
711 *Physiol.*, 16, 61-68.
712

713 Cienciala, E., Lindroth, A., 1995. Gas-exchange and sap flow measurements of *Salix viminalis*
714 trees in short-rotation forest. II: Diurnal and seasonal variations of stomatal response and water
715 use efficiency. *Trees*, 9, 295-301.
716

717 Cienciala, E., 1994. Sap flow, transpiration and water use efficiency of spruce and willow in
718 relation to climatic factors. Swedish University of Agricultural Sciences, Uppsala, Sweden, PhD
719 Thesis, 120 pp.
720

721 Crago, R.D., Brutsaert, W., 1996. Daytime evaporation and the self-preservation
722 of the evaporative fraction and the Bowen ratio. *Journal of hydrology.*, 178, 241-255.
723

724 Domec, J.S., Johnson, D.M., 2012. Does homeostasis or disturbance of homeostasis in minimum
725 leaf water potential explain the isohydric versus anisohydric behavior of *Vitis vinifera* L.
726 cultivars? *Tree Physiol.*, 32, 245-248.
727

728 Dyer, A.J., Hicks, B.B., 1970. Flux-gradient relationships in the constant flux layer. *Quart. J.*
729 *Roy. Meteorol. Soc.*, 96, 715-721.
730

731 Eisentraut, A., 2010. Sustainable Production of Second-Generation Biofuels. © OECD/IEA
732 Report. Available at: <http://ideas.repec.org/p/oec/ieaaaa/2010-1-en.html>.
733

734 European Parliament and EU Council, Directive 2009/28/EC (23 April 2009) on the Promotion
735 of the Use of Energy from Renewable Sources. Official Journal of the European Union L 140
736 (EN): 16–62..
737

738 Falge, E., Baldocchi, D., Tenhunen, J., Aubinet, M., Bakwin, P., Berbigier, P., Bernhofer, C.,
739 Burba, G., Clement, R., Davis, K.J., Elbers, J.A., Goldstein, A.H., Grelle, A., Granier, A.,
740 Guðmundsson, J., Hollinger, D., Kowalski, A.S., Katul, G., Law, B.E., Malhi, Y., Meyers, T.,
741 Monson, R.K., Munger, J.W., Oechel, W., U, K.T.P., Pilegaard, K., Rannik, Ü., Rebmann, C.,
742 Suyker, A., Valentini, R., Wilson, K., Wofsy, S., 2002. Seasonality of ecosystem respiration and
743 gross primary production as derived from FLUXNET measurements. *Agric. For. Meteorol.*, 113,
744 53-74.

745

746 Fischer, M., 2012. Water balance of short rotation coppice. Mendel University in Brno, Czech
747 Republic, Ph.D thesis, 261 pp.

748

749 Fischer, M., Trnka, M., Kučera, J., Deckmyn, G., Orság, M., Sedlák, P., Žalud, Z., Ceulemans,
750 R., 2013. Evapotranspiration of a high-density poplar stand in comparison with a reference grass
751 cover in the Czech–Moravian Highlands. *Agric. For. Meteorol.*, 181, 43-60.

752

753 Foken, T., Wichura, B., 1996. Tools for quality assessment of surface-based flux 880
754 measurements. *Agric. For. Meteorol.*, 78, 83-105.

755

756 Foken, T., 2008. The energy balance closure problem - an overview. *Ecol. Appl.*, 18, 1351-1367.

757

758 Foken, T., Leuning, R., Oncley, S.R., Mauder, M., Aubinet, M., 2012. Corrections and data
759 quality control. In: Aubinet, M., Vesala, T., Papale, D., (Eds.) *Eddy covariance: A practical
760 guide to measurement and data analysis*. Springer, London, UK, 438 pp.

761

762 Foken, T., Göckede, M., Mauder, M., Mahrt, L., Amiro, B., Munger, J.W., 2004. Postfield
763 data quality control. In *Handbook of Micrometeorology, A Guide for Surface Flux Measurement
764 and Analysis* (eds Lee, X., et al.) pp 181-208, Kluwer Academic Publisher Dordrecht, The
765 Netherlands.

766

767 Fratini, G., Ibrom, A., Arriga, N., Burba, G., Papale, D., 2012. Relative humidity effects on
768 water vapour fluxes measured with closed-path eddy-covariance systems with short sampling
769 lines. *Agric. For. Meteorol.*, 165, 53-63.

770

771 Gentine, P., Entekhabi, D., and Polcher, J., 2011. The Diurnal Behavior of Evaporative Fraction
772 in the Soil–Vegetation–Atmospheric Boundary Layer Continuum. *J. Hydrometeorol.*, 12, 1530-
773 1546.

774

775 Guidi, W., Piccioni, E., Bonari, E., 2008. Evapotranspiration and crop coefficient of
776 poplar and willow short-rotation coppice used as vegetation filter. *Bioresour.
777 Technol.*, 99, 4832-4840.

778

779 Hall, R.L., Allen, S.J., Rosier, P.T.W., et al., 1996. Hydrological effects of short rotation energy
780 coppice. ETSU B/W5/00275/REP. ETSU Technical Report for DTI. Harwell, 226 p.

781

782 Hall, R.L., Allen, S.J., Rosier, P.T.W Hopkins, R., 1998. Transpiration from coppiced
783 poplar and willow measured using sap flow methods. *Agric. For. Meteorol.*, 90, 275-290.

784 Heim, R.R., 2002. A review of twentieth-century drought indices used in the United States. Bull.
785 Am. Meteorol. Soc., 83, 1149-1165.
786
787 Herbst, M., 1995. Stomatal behaviour in a beech canopy: an analysis of Bowen ratio
788 measurements compared with porometer data. Plant, Cell Environ., 18, 1010-1018.
789
790 Hinckley, T.M., Brooks, J.R., Cermak, J., Ceulemans, R., Kucera, J., Meinzer, F.C., Roberts,
791 D.A., 1994. Water flux in a hybrid poplar stand. Tree Physiol., 14,1005-1018.
792
793 Houghton, J.T., Meira Filho, L.G., Callander, B.A., Harris, N., Kattenberg, A., Maskell, K. Eds.
794 1996. Climate Change 1995—The Science of Climate Change. Cambridge University
795 Press, Cambridge. UK 572 pp
796
797 Horst, T., 1997. A simple formula for attenuation of eddy fluxes measured with first order-
798 response scalar sensors. Boundary-Layer Meteorol., 82, 219-233.
799
800 Ingwersen, J., Steffens, K., Högy, P., Warrach-Sagi, K., Zhunusbayeva, D., Poltoradnev, M.,
801 Gäbler, R., Wizemann, H.D., Fangmeier, A., Wulfmeyer, V., Streck, T., 2011. Comparison of
802 NOAH simulations with eddy covariance and soil water measurements at a winter wheat stand.
803 Agric. For. Meteorol., 151, 345-355.
804
805 Iritz, Z., Lindroth, A., 1996. Energy partitioning in relation to leaf area development of short-
806 rotation willow coppice. Agric. For. Meteorol., 81, 119-130.
807
808 Iritz, Z., Tourula, T., Lindroth, A., Heikinheimo, M., 2001. Simulation of willow short-rotation
809 forest evaporation using a modified Shuttleworth–Wallace approach. Hydrol. Processes, 15, 97-
810 113.
811
812 Jarvis, P.G., McNaughton, K.G., 1986. Stomatal control of transpiration: scaling up from leaf to
813 region. Adv. Ecol. Res., 15, 1-49.
814
815 Khamzina, A., Sommer, R., Lamers, J.P.A., Vlek, P.L.G., 2009. Transpiration and early growth
816 of tree plantations established on degraded cropland over shallow saline groundwater table in
817 northwest Uzbekistan. Agric. For. Meteorol., 149, 1865-1874.
818
819 Kauter, D., Lewandowski, I., Claupain, W., 2003. Quantity and quality of harvestable biomass
820 from *Populus* short rotation coppice for solid fuel use: a review of the physiological basis and
821 management influences. Biomass Bioenergy, 24, 411-427.
822
823 Keyser, A.R., Kimball, J.S., Nemani, R.R., Running, S.W., 2000. Simulating the effects of
824 climate change in the carbon balance of North American high-latitude forests. Global Change
825 Biol., 6, 185-195.
826
827 Kim, H.S., Oren, R., Hinckley, T.M., 2008. Actual and potential transpiration and carbon
828 assimilation in an irrigated poplar plantation. Tree Physiol., 28, 559-577.
829

830 King, J.S., Ceulemans, R., Albaugh, J.M., Dillen, S.Y., Domec, J-C., Fichot, R., Fischer, M.,
831 Leggett, Z., Sucre, E., Trnka, M., Zenone, T., 2013. The challenge of ligno-cellulosic
832 bioenergy in a water-limited world. *BioScience*, 63, 102-117.
833

834 Lasch, P., Kollas, C., Rock, J., Suckow, F., 2010. Potentials and impacts of short rotation
835 coppice plantation with aspen in Eastern Germany under conditions of climate change. *Reg.*
836 *Environ. Change*, 10, 83-94.
837

838 Liberloo, M., Calfapietra, C., Lukac, M., Godbold, D., Luo, Z.B., Polle, A., Hoosbeck, M.R.,
839 Kull, O., Marek, M., Raines, C., Rubino, M., Taylor, G., Scarascia-Mugnozza, G., Ceulemans,
840 R., 2006. Woody biomass production during the second rotation of a bio-energy *Populus*
841 plantation increases in a future high CO₂ world. *Global Change Biol.*, 12, 1094-1106.
842

843 Lindroth, A., 1993. Aerodynamic and canopy resistance of short-rotation forest in relation to leaf
844 area index and climate. *Boundary-Layer Meteorol.*, 66, 265-279.
845

846 Lindroth, A., Verwijst, T., Halldin, S., 1994. Water-use efficiency of willow: variation
847 with season, humidity and biomass allocation. *J. Hydrol.*, 156, 1-19.
848

849 Liu, S., Mao, D., Lu, L., 2007. Measurement and estimation of the aerodynamic resistance.
850 *Hydrology Earth Syst. Sci.* 11, 769-783.
851

852 Migliavacca, M., Meroni, M., Manca, G., *et al.*, 2009. Seasonal and interannual patterns of
853 carbon and water fluxes of a poplar plantation under peculiar eco-climatic conditions. *Agric. For.*
854 *Meteorol.*, 149, 1460-1476.
855

856 Moffat, A.M., Papale, D., Reichstein, M., *et al.*, 2007. Comprehensive comparison of gap-filling
857 techniques for eddy covariance net carbon fluxes. *Agric. For. Meteorol.*, 147, 209-232.
858

859 Monteith, J.L., Unsworth, M.H., 2013. *Principles of Environmental Physics: Plants, Animals,*
860 *and the Atmosphere*. 4th edition Academic Press, London, UK, 401 pp.
861

862 Mauder, M., Foken, T., 2006. Impact of post-field data processing on eddy covariance flux
863 estimates and energy balance closure. *Meteorol. Zeitschrift*, 15, 597-609.
864

865 Munger, J.W., Loescher, H.W., Luo, H., 2012. Measurements, tower and site design
866 considerations. In: Aubinet M, Vesala T, Papale D (Eds.) *Eddy Covariance: A Practical Guide to*
867 *Measurement and Data Analysis*. Springer, London, UK, 438 pp.
868

869 Neumann, D.S., Wagner, M., Braatne, J.H., Howe, J., 1996. Stress physiology—abiotic. In:
870 Stettler RF, Bradshaw HD, Heilman PE, Hinckley TM (eds) *Biology of Populus and its*
871 *Implications for Management and Conservations*. Research Press. Ottawa, Ontario, Canada.
872 423-449 pp
873

874 Oren, R., Sperry, J.S., Katul, G.G., Pataki, D.E., Ewers, B.E., Philips, N., Schäfer, K.V.R., 1999.
875 Survey and synthesis of intra- and interspecific variation in stomatal sensitivity to vapour
876 pressure deficit. *Plant, Cell Environ.*, 22, 1515-1526.
877

878 Papale, D., Reichstein, M., Aubinet, M., 2006. Towards a standardized processing of net
879 ecosystem exchange measured with eddy covariance technique: algorithms and uncertainty
880 estimation. *Biogeosciences*, 3, 571-583.
881

882 Peng, J., Borsche, M., Liu, Y., Loew, A., 2013. How representative are instantaneous
883 evaporative fraction measurements of daytime fluxes? *Hydrol. Earth Syst. Sci.*, 17 (10), 3913-
884 3919.
885

886 Perry, C.H., Miller, R.C., Brooks, K.N., 2001. Impacts of short-rotation hybrid poplar
887 plantations on regional water yield. *Forest Ecology Manag.*, 143,143-151.
888

889 Petzold, R., Schwärzel, K., Feger, K.H., 2010. Transpiration of a hybrid poplar plantation
890 in Saxony (Germany) in response to climate and soil conditions. *Eur. J. For. Res.* 130, 695-706.
891

892 Pita, G., Gielen, B., Zona, D., Rodrigues, A., Rambal, S., Janssens, I.A., Ceulemans, R., 2013.
893 Carbon and water vapor fluxes over four forests in two contrasting climatic zones. *Agric. For.*
894 *Meteorol.*, 180, 211-224.
895

896 Priestley, C.H.B., Taylor, R.J., 1972. On the assessment of surface heat flux and evaporation
897 using large-scale parameters. *Mon. Weather Rev.*, 100, 81-92.
898

899 Randerson, J.T., Field, C.B., Fung, I.Y., Tans, P.P., 1999. Increases in early season ecosystem
900 uptake explain recent changes in the seasonal cycle of atmospheric CO₂ at high northern
901 latitudes. *Geophys. Res. Lett.*, 26, 2765–2768.
902

903 Reichstein, M., Tenhunen, J.D., Rouspard, O., Ourcival, J.M., Rambal, S., Miglietta, F.,
904 Peressotti, A., Pecchiari, M., Tirone, G., Valentini, R., 2002. Severe drought effects on
905 ecosystem CO₂ and H₂O fluxes at three Mediterranean evergreen sites: revision of current
906 hypotheses? *Global Change Biol.*, 8, 999-1017.
907

908 Reichstein, M., Falge, E., Baldocchi, D., Papale, D., Aubinet, M., Berbigier, P., Bernhofer, C.,
909 Buchmann, N., Gilmanov, T., Granier, A., Grünwald, T., Havránková, K., Ilvesniemi, H.,
910 Janous, D., Knohl, A., Laurila, T., Lohila, A., Loustau, D., Matteucci, G., Meyers, T., Miglietta,
911 F., Ourcival, J.M., Pumpanen, J., Rambal, S., Rotenberg, E., Sanz, M., Tenhunen, J., Seufert, G.,
912 Vaccari, F., Vesala, T., Yakir, D., Valentini, R., 2005. On the separation of net ecosystem
913 exchange into assimilation and ecosystem respiration: Review and improved algorithm. *Global*
914 *Change Biol.*, 11, 1424-1439.
915

916 San Miguel-Ayanz, J., Vogt, J., De Roo, A., Schmuck, G., 2000. Natural hazards monitoring:
917 forest fires, droughts and floods – the example of European pilot projects. *Surv. Geophys.*, 21,
918 291-305.
919

920 Shuttleworth, W.J., 2007. Putting the ‘vap’ into evaporation. *Hydrology Earth Syst. Sci.*, 11,
921 210-244.

922

923 Schwalm, C.R., Williams, C.A., Schaefer, K., Arneth, A., Bonal, D., Buchmann, N., Chen, J.,
924 Law, B., Lindroth, A., Luysaert, S., Reichstein, M., Richardson, A.D., 2010. Assimilation
925 exceeds respiration sensitivity to drought: A FLUXNET synthesis. *Global Change Biol.*, 16, 657-
926 670.

927

928 Schmidt-Walter, P., Richter, F., Herbst, M., Schuldt, B., Lamersdorf, N.P., 2014. Transpiration
929 and water use strategies of a young and a full-grown short rotation coppice differing in canopy
930 cover and leaf area. *Agric. For. Meteorol.*, 195-196, 165-178.

931

932 Schmid, H.P., Grimmond, C.S.B., Cropley, F., Offerle, B., Su, H.B., 2000. Measurements of
933 CO₂ and energy fluxes over a mixed hardwood forest in the mid-western United States. *Agric.*
934 *For. Meteorol.*, 103, 357-374.

935

936 Stull, R.B. 1988. *Introduction to Boundary-Layer Meteorology*. Kluwer Academic publisher.
937 Dordrecht. The Netherlands. 666 pp.

938

939 Sugita, M., Brutsaert, W., 1991. Daily evaporation over a region from lower boundary layer
940 profiles measured with radiosondes. *Water Resour. Res.*, 27, 747-752.

941

942 Thom, A.S., 1972. Momentum, mass and heat exchange of vegetation. *Quart. J. Roy. Meteorol.*
943 *Soc* 98, 124-134.

944

945 Tricker, P.J., Pecchiari, M., Bunn, S.M., Vaccari, F.P., Peressotti, A., Miglietta, F., Taylor, G.,
946 2009. Water use of a bioenergy plantation increases in a future high CO₂ world. *Biomass*
947 *Bioenergy* 33(2), 200-208.

948

949 Verlinden, M.S., Broeckx, L.S., Van den Bulcke, J., Van Acker, J., Ceulemans, R., 2013.
950 Comparative study of biomass determinants of 12 poplar (*Populus*) genotypes in a high-density
951 short-rotation culture. *Forest Ecol. Manag.*, 307, 101-111.

952

953 Webb, E.K., Pearman, G.I., Leuning, R., 1980. Correction of flux measurements for 1056
954 density effects due to heat and water-vapor transfer. *Quart. J. Roy. Meteorol. Soc.*, 106, 85-100.

955

956 Wilson, K.B., Baldocchi, D.D., 2000. Seasonal and interannual variability of energy fluxes over
957 a broadleaved temperate deciduous forest in North America. *Agric. For. Meteorol.*, 100, 1-18.

958

959 Wilson, K.B., Baldocchi, D.D., Aubinet, M., Berbigier, P., Bernhofer, C., Dolman, H., Falge, E.,
960 Field, C., Goldstein, A., Granier, A., Grelle, A., Halldor, T., Hollinger, D., Katul, G., Law, B.E.,
961 Lindroth, A., Meyers, T., Moncrieff, J., Monson, R., Oechel, W., Tenhunen, J., Valentini, R.,
962 Verma, S., Vesala, T., Wofsy, S., 2002. Energy partitioning between latent and sensible heat flux
963 during the warm season at FLUXNET sites. *Water Resour. Res.* 38, 30-1–30-11.

964

965 Wilson, K.B., Goldstein, A., Falge, E., Aubinet, M., Baldocchi, D., Berbigier, P., Bernhofer, C.,
966 Ceulemans, R., Dolman, H., Field, C., Grelle, A., Ibrom, A., Law, B.E., Kowalski, A.,
967 Meyers, T., Moncrieff, J., Monson, R., Oechel, W., Tenhunen, J., Valentini, R., Verma, S.,
968 2002b. Energy balance closure at FLUXNET sites. *Agric. For. Meteorol.* 113, 223-243.
969
970 Wohlfahrt, G., Haslwanter, A., Hörtnagl, L., Jasoni, R.L., Fenstermaker, L.F., Arnone III, J.,
971 Hammerle, A., 2009. On the consequences of the energy imbalance for calculating surface
972 conductance to water vapour. *Agric. For. Meteorol.*, 149, 1556-1559.
973
974 Zetterberg, L., Chen, D., 2014. The time aspect of bioenergy – climate impacts of solid biofuels
975 due to carbon dynamics. *GCB Bioenergy*. doi: 10.1111/gcbb.12174.
976
977 Zona, D., Janssens, I.A., Aubinet, M., Gioli, B., Vicca, S., Fichot, R., Ceulemans, R., 2013.
978 Fluxes of the greenhouse gases (CO₂, CH₄ and N₂O) above a short-rotation poplar plantation
979 after conversion from agricultural land., *Agric. For. Meteorol.*, 169, 100-110.
980
981
982
983
984
985
986
987
988
989
990
991
992
993
994
995
996
997
998
999

	LAI 0-1					LAI 4-6				1000
	constant	B	SE B	β	R^2	constant	B	SEB	β	R^2
Rg	25.61	0.33	0.01	.79*	0.62	36.71	0.48	0.01	.87*	0.77
Air T	-31.6	6.72	0.55	.35*	0.13	-107.85	12.86	0.6	0.51*	0.37
VPD	102.12	32.16	6.48	.26*	0.07	131.52	72.75	10.46	.32*	0.10

1003

1004 Table 1 Regression coefficients of the relationship between latent heat (LE) (dependent variable)
 1005 and net radiation (Rg), air temperature (Air T) and vapor pressure deficit (VPD (predictors) for
 1006 two levels of leaf area index (LAI).

1007 * $p < .05$

1008

1009

1010

1011

1012

1013

1014

1015

1016

1017

1018

1019

1020

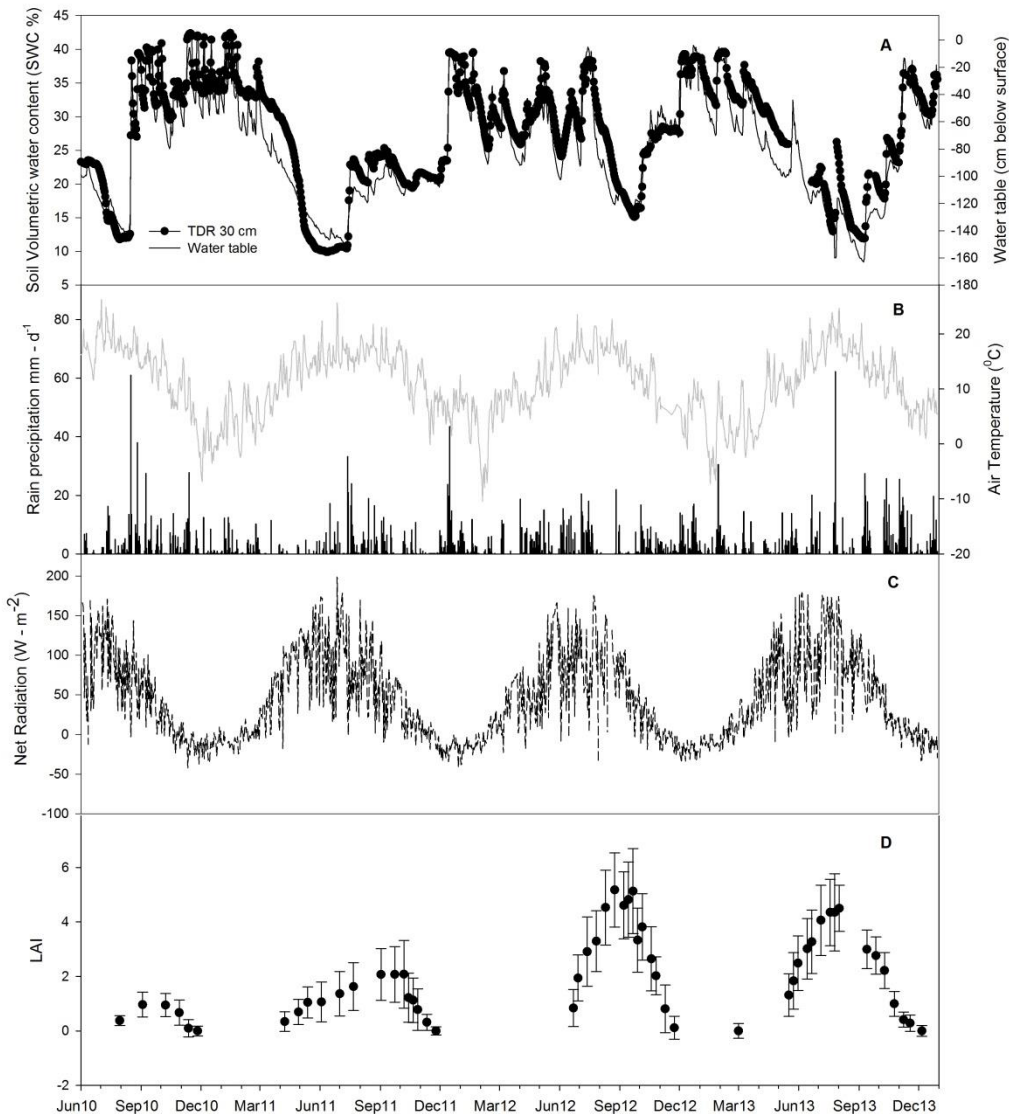
1021

1022

1023

1024

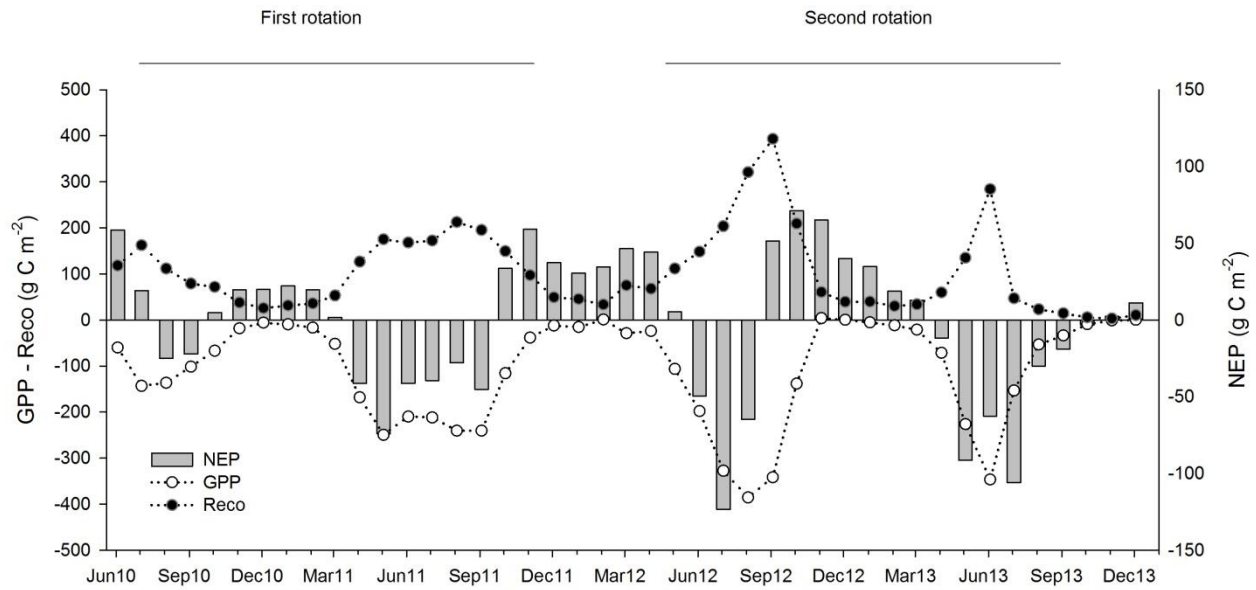
1025



1026

1027 Fig. 1 Evolution of different environmental parameters and leaf area index (LAI) during the
 1028 course of the four growing seasons of the short-rotation poplar plantation. Panel A: daily average
 1029 temporal trend of the water table depth and volumetric soil water content (% as measured with
 1030 TDR). Panel B: mean daily air temperature (°C) and precipitation (mm d⁻¹). Panel C: daily
 1031 average net radiation. Panel D: seasonal distribution of leaf area index (LAI): measurements
 1032 (data points) represent the average of the 12 clones of the plantation and vertical bars represent
 1033 the standard deviation.

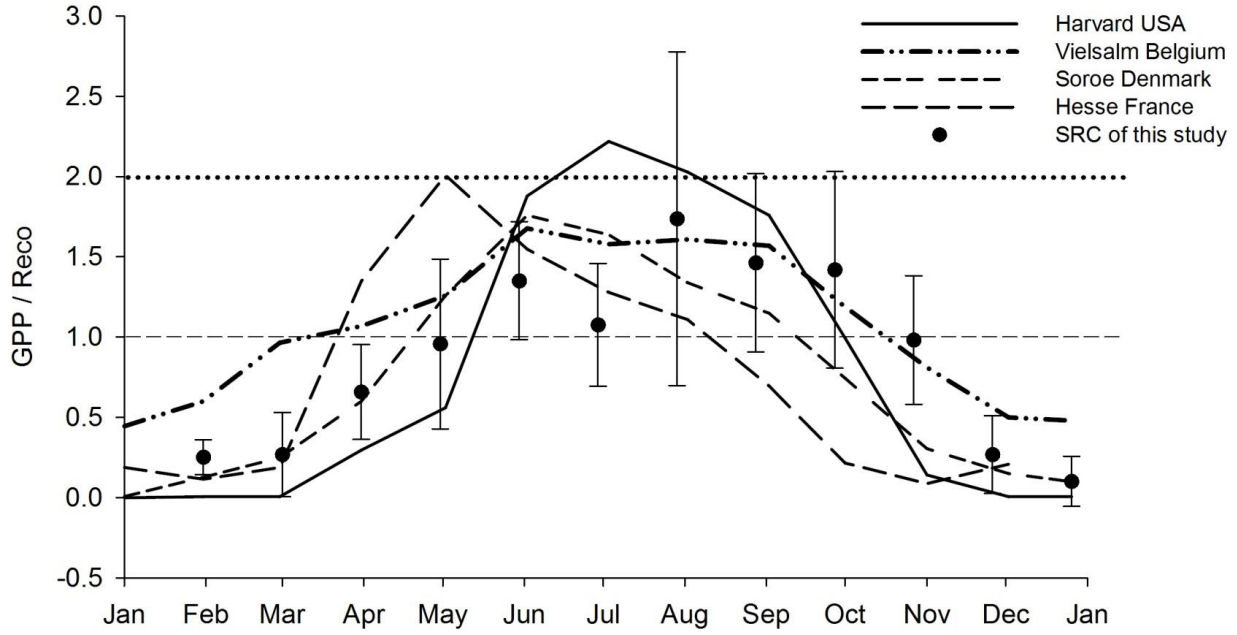
1034



1035

1036 Fig. 2 Seasonal dynamics of the monthly cumulative gross primary production (GPP), ecosystem
 1037 respiration (R_{eco}) and net ecosystem production (NEP) during the two rotations (four years) of
 1038 the short-rotation coppice plantation.

1039
 1040
 1041
 1042
 1043
 1044
 1045
 1046
 1047
 1048
 1049
 1050
 1051
 1052
 1053
 1054
 1055
 1056
 1057
 1058
 1059
 1060
 1061
 1062
 1063
 1064



1065
1066

1067 Fig.3 Annual dynamics of the gross primary production and ecosystem respiration ratio
 1068 (GPP/Reco) at the study site as compared to a series of deciduous forests reported by Falge et al.
 1069 (2002). An GPP/Reco value of 1 (dashed line) indicates that the cumulative net ecosystem
 1070 exchange (NEE) was equal to 0. The value of 2 (dotted line) corresponds to the cumulative NEE
 1071 begin equal to Reco, indicating a low overall contribution of the heterotrophic respiration.
 1072

1073

1074

1075

1076

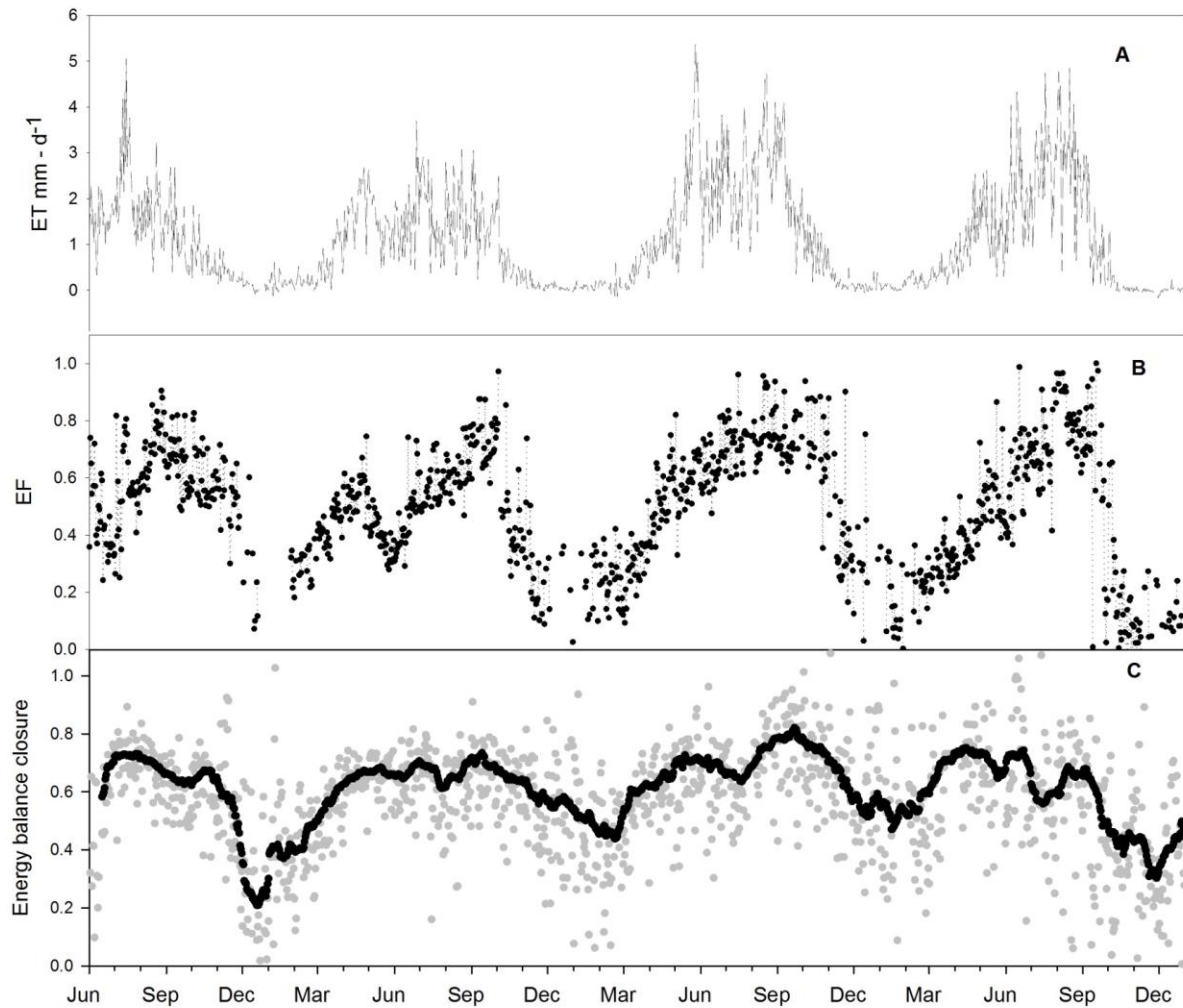
1077

1078

1079

1080

1081



1082

1083 Fig. 4 Panel A: Temporal dynamics of the daily evapotranspiration totals (ET). Panel B: midday
 1084 average evaporative fraction (EF) as a measure of energy partitioning and as an indicator of
 1085 eventual drought episodes calculated for midday periods from 11:00 to 14:00. Panel C: temporal
 1086 variation of the energy balance closure using non-gap-filled data. The gray points represent the
 1087 daily linear regression slopes of the relationship between available energy ($R_n - G$) and eddy-
 1088 covariance energy fluxes ($H + LE$). The black points represent the slopes of a running window of
 1089 30 days. H = sensible heat, LE = latent heat, G = soil heat flux, R_n = net radiation.

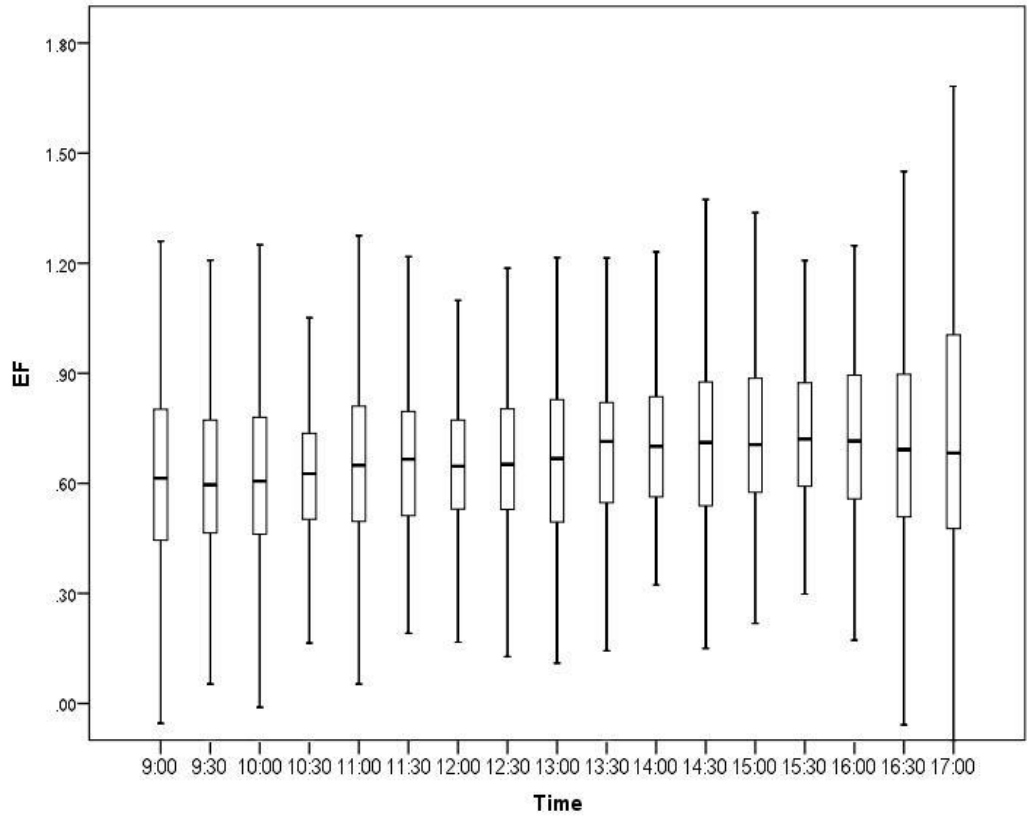
1090

1091

1092

1093

1094



1095

1096 Fig. 5 Box plots of the daily trend of the evaporative fraction (EF) measured during the 2013
 1097 growing season. Each box covers the interquartile range (50% of the scores); the median value is
 1098 drawn as a horizontal black line, and the whiskers indicate the bottom and top quartile.
 1099

1100

1101

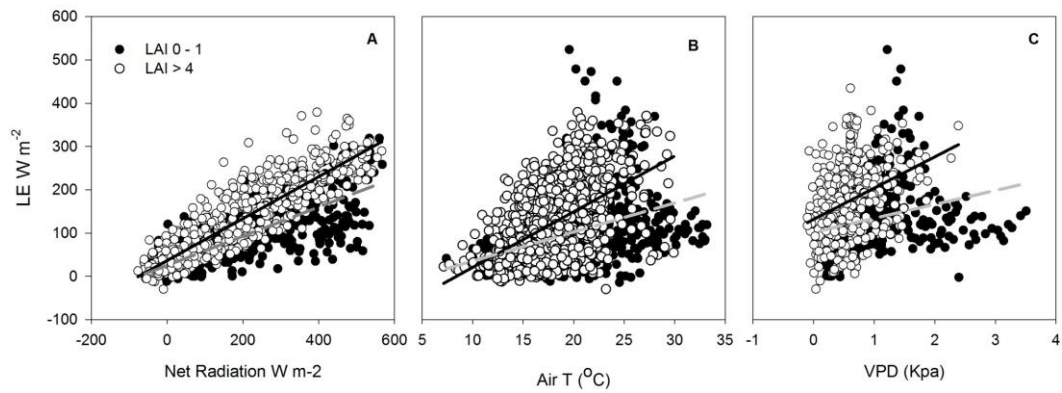
1102

1103

1104

1105

1106



1107

1108 Fig. 6 Relationship between latent heat (LE) and net radiation (R_n ; panel A), air temperature (Air
 1109 T) (panel B) and vapour pressure deficit (VPD; panel C) at two levels of LAI: 0-1 (black circles)
 1110 and LAI > 4 (white circles). LAI = Leaf area index

1111

1112

1113

1114

1115

1116

1117

1118

1119

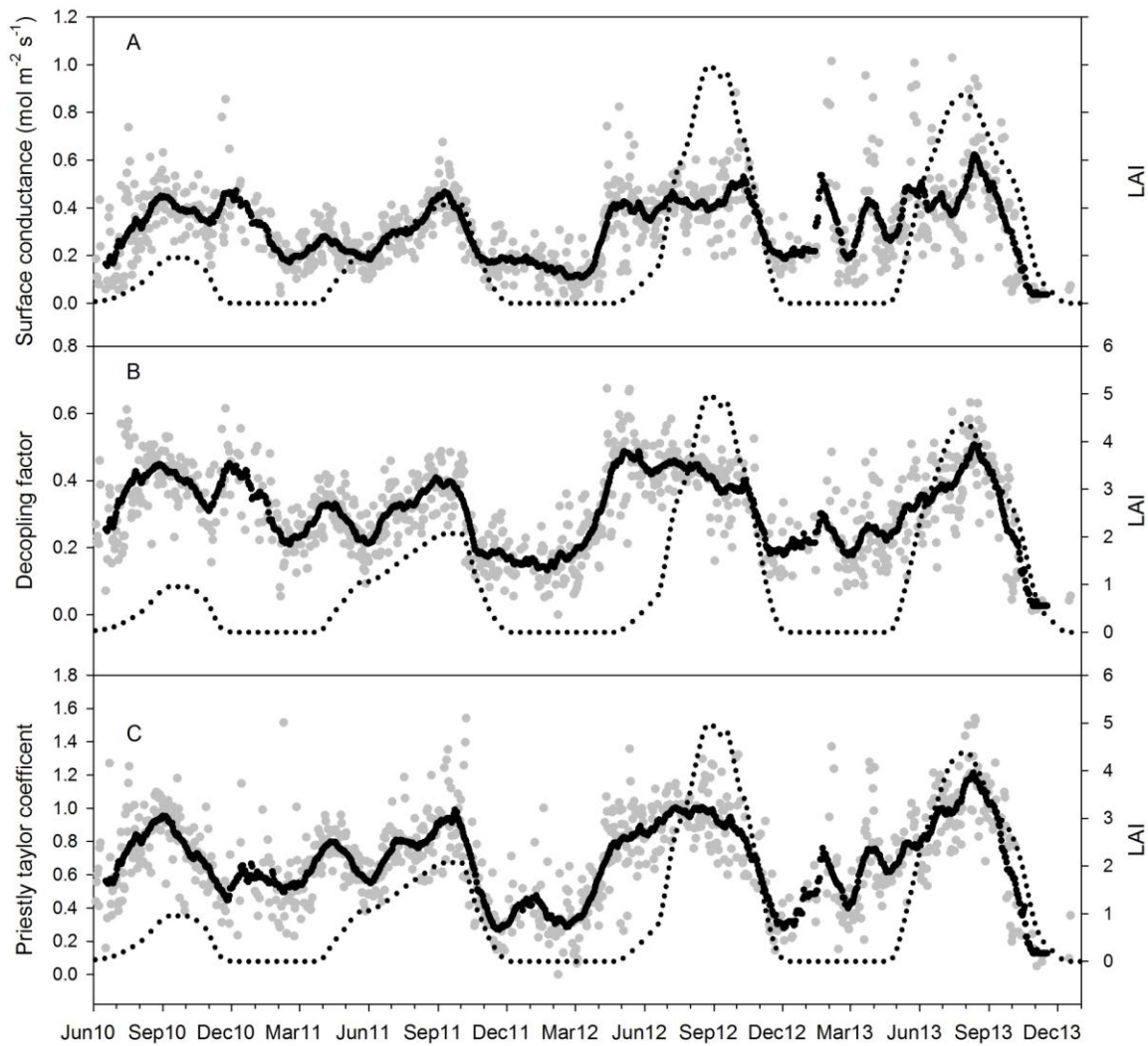
1120

1121

1122

1123

1124



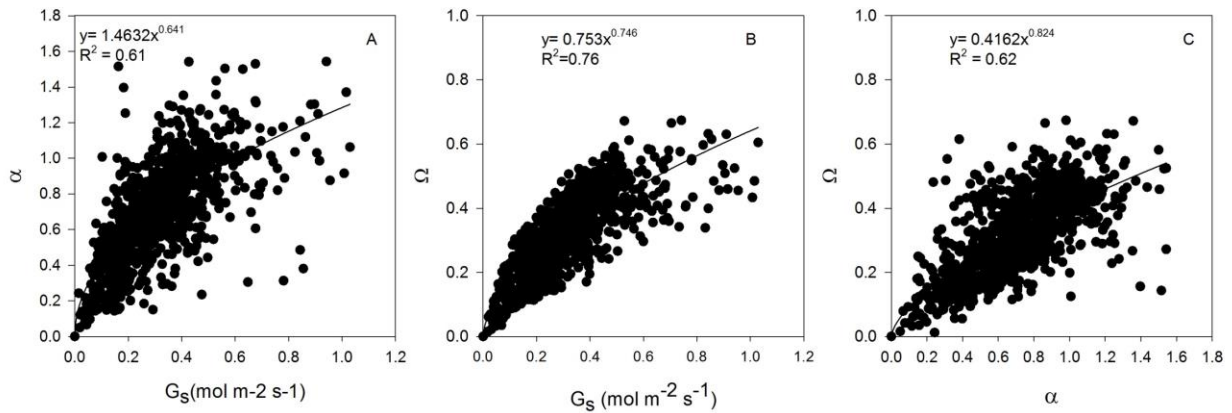
1125

1126 Fig. 7. Temporal variation of surface conductance (A), decoupling factor (B) and Priestley-
 1127 Taylor coefficient (C) expressed as daily means weighted by net radiation (gray points). Data are
 1128 calculated from half-hourly diurnal values during conditions with a dry canopy. The days when
 1129 less than 30% of the diurnal values were available were excluded from the analysis. The black
 1130 solid line expresses the 30-day running mean calculated from the daily values. The dashed black
 1131 lines depict the leaf area index (LAI).

1132

1133

1134



1135

1136 Fig. 8. Scatter plot relationships between surface conductance (G_s) and Priestley-Taylor
 1137 coefficient (panel A), surface conductance and decoupling factor (panel B), and Priestley-Taylor
 1138 coefficient and decoupling factor (panel C). The points represent daily means of diurnal values
 1139 for dry surface conditions weighted by net radiation. The days when less than 30% of diurnal
 1140 values were available were excluded from the analysis.

1141

1142

1143

1144

1145

1146

1147

1148

1149

1150

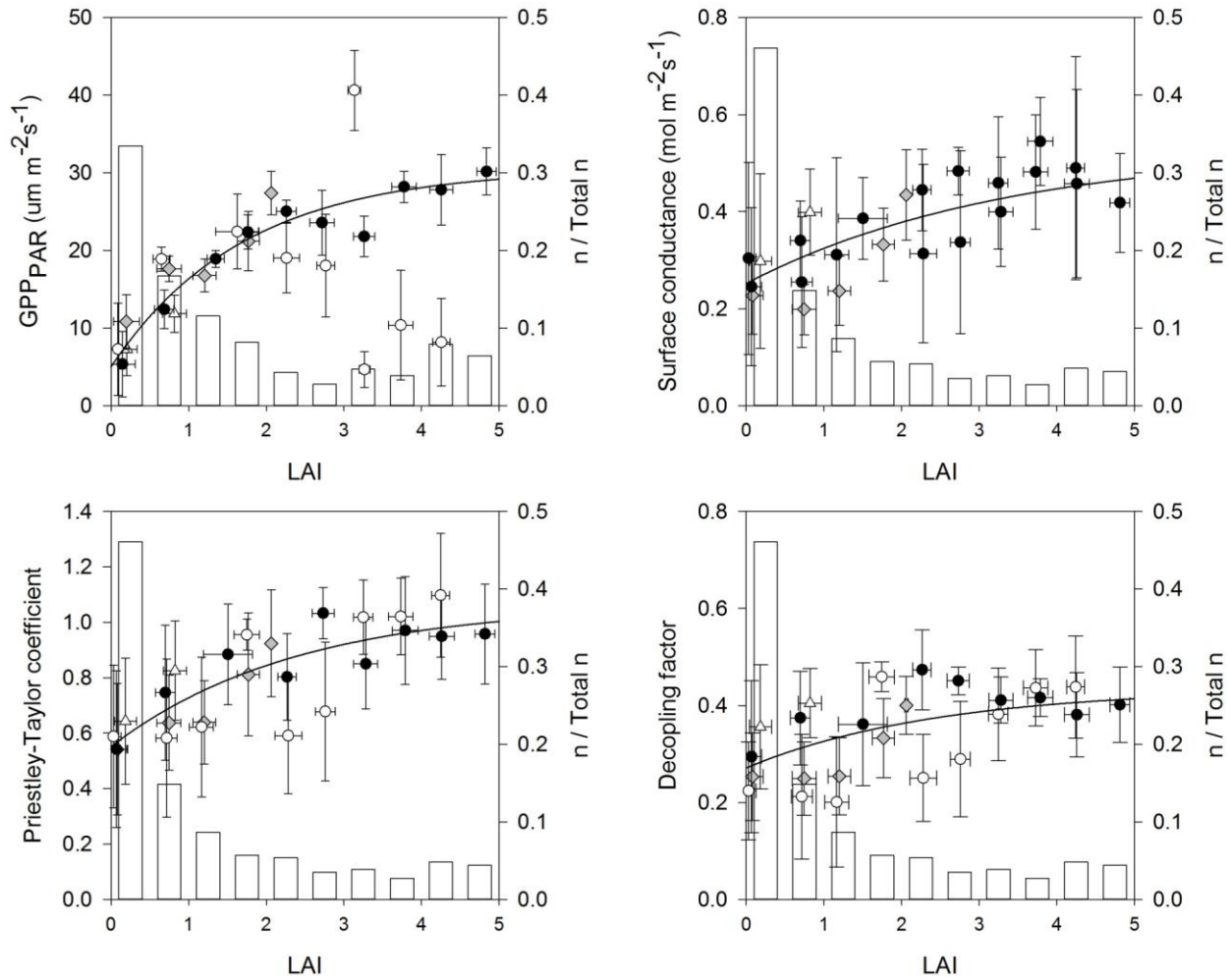
1151

1152

1153

1154

1155

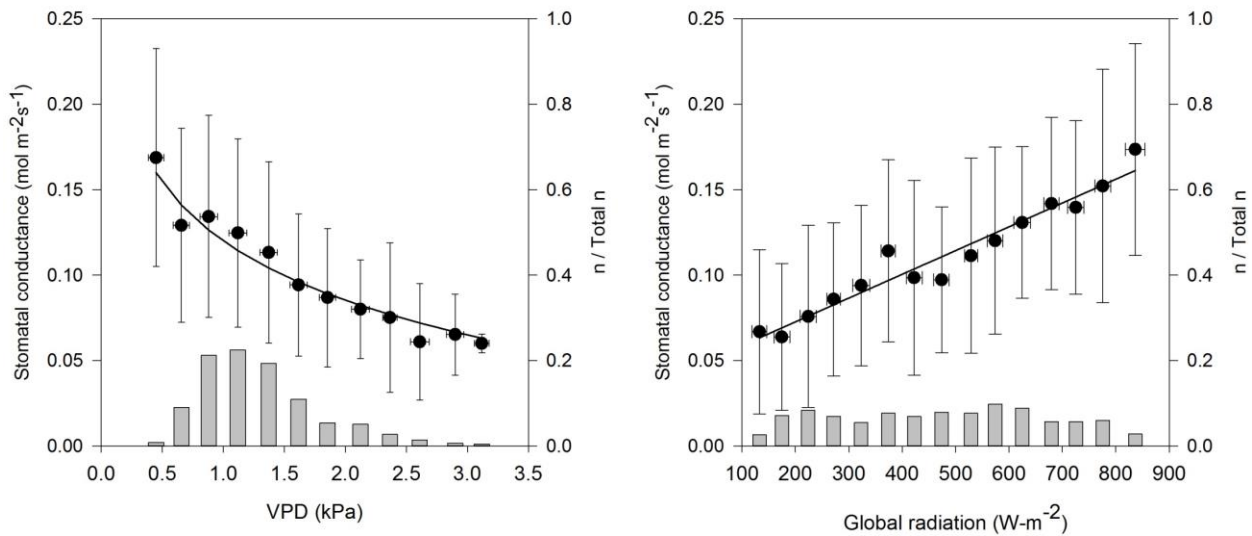


1156

1157 Fig. 9 Relationships between leaf area index (LAI) and gross primary productivity (GPP)
 1158 described by the function $GPP_{PAR} = 30.55 - 25.52 \cdot \text{EXP}(-0.58 \cdot \text{LAI})$ $R^2 = 0.76$ (A); surface
 1159 conductance and leaf area index described by the function $G_s = 0.53 - 0.28 \cdot \text{EXP}(-0.3 \cdot \text{LAI})$, $R^2 =$
 1160 0.18 (B); Priestley-Taylor coefficient versus leaf area index described by the function $\alpha = 1.06 -$
 1161 $0.51 \cdot \text{EXP}(-0.42 \cdot \text{LAI})$ $R^2 = 0.30$ (C); and decoupling factor and leaf area index expressed by the
 1162 function $\Omega = 0.43 - 0.16 \cdot \text{EXP}(-0.41 \cdot \text{LAI})$ $R^2 = 0.14$ (D). All of the parameters were statistically
 1163 significant ($p < 0.0001$). The points represent the averages of daily values binned according to
 1164 leaf area index ($0.5 \text{ m}^2 \text{ m}^{-2}$). White triangles: season 2010; gray diamonds = 2011; black circles =
 1165 2012 and white circles = 2013. The error lines indicate the standard deviation. The white vertical
 1166 bars show the frequency distribution. Daily means are calculated from diurnal half-hourly values
 1167 during conditions with a dry canopy and weighted by net radiation. The days when less than 30%
 1168 of diurnal values were available were excluded from the analysis. In case of GPP, four
 1169 distinctive outliers representing 37 days in summer 2013 were excluded for fitting the function.

1170

1171



1172

1173 Fig. 10: Relationship between vapor pressured deficit (VPD) and mean stomatal conductance
 1174 (g_s) for light saturated conditions (global radiation $> 500 \text{ W m}^{-2}$) (left panel, A). The particular
 1175 points express the averages of the half-hour values binned according to VPD (0.25 kPa).
 1176 Relationship between global radiation and reference mean g_s (right panel, B). Points represent
 1177 the averages of half-hourly values binned according to global radiation (50 W m^{-2}). The
 1178 reference mean g_s was calculated in narrow range of vapor pressure deficit between 0.9 to 1.1
 1179 kPa. Mean g_s is represented by the surface conductance divided by the leaf area index (LAI)
 1180 during dry canopy conditions when LAI exceeded 3. The error lines indicate the standard
 1181 deviation and the gray vertical bars show the frequency distribution.

1182